2-23-1992

Dynamic analysis of an electromagnetic shutter system

Peter Newman

Dynamic Analysis of an Electromagnetic Shutter System

Peter Newman

A Thesis submitted in partial fulfillment of the requirements for the
Degree of Master of Science in Mechanical Engineering,
Rochester Institute of Technology,
Rochester, New York.

Approved by:

Dr. J. S. Torok (Advisor)

Dr. H. Ghoneim

Dr. M. H. Kempski

Dr. C. Haines (Department Head)

February 23, 1992

I, Peter Newman, do hereby grant Wallace Memorial Library permission to reproduce my thesis in whole or in part. Any reproduction by Wallace Memorial Library will not be used for commercial use or profit.

Abstract

This report presents a method of analysis that may be applied to dynamical systems operating in electromagnetic fields. The investigation focuses in particular on the dynamic response of an electromagnetic shutter system. A derivation of Finite Element Analysis applied to magnetostatics is reviewed. An introduction to photographic exposure calculations is also reviewed. The shutter system is broken down into three models for analysis: a magnetic model, a mechanical model, and a photometric model. The equations of motion are derived, based on the electromagnetic field calculations. The governing equations are analyzed using the Advanced Continuous Simulation Language (ACSL) software, and the uses for the model are discussed.

Acknowledgements

I would like to thank my advisor, Dr. Joe S. Torok, for his help and guidance.

I appreciate the time Dr. Ed Furlani took to discuss the derivation of magnetic field energy with me and to provide the field energy solutions.

Special thanks to David R. Dowe for designing the shutter mechanism.

I would like to thank Dr. J. Kelly Lee and Beth O'Leary for their comments on the manuscript. I appreciate the support Dr. Ed Walsh has shown on this project.

I would like to recognize my colleagues at work for encouraging me to finish the thesis.

I am especially grateful to my wife, Mila for her encouragement and helpful suggestions.

Table of Contents

I Introduction 1

II Literature Review 4

Electromagnetic Field Solutions 4

Field Solutions including Permanent Magnets 5

Magnetic Force Calculation 6

Dynamics of Mechanisms 6

Dynamic Performance of Electromechanical Systems 7

III Electromagnetic Field Theory 8

Maxwell's Equations - Magnetostatics 8

Magnetic Materials 10

Two Dimensional Magnetic Vector Potential 13

Solution of the Vector Potential 15

Approximate Solution 19

Field Energy 21

Magnetic Force Calculation 23

IV Exposure Calculations 24

Shutter Speed 25

Aperture 26

Exposure Value 27

Brightness 27

Film Speed 28

Exposure Adjustment 28

Shutter Characteristics 29

V Shutter Model 31

Shutter Description 31

Magnetic Model of the Shutter 32

Mechanical Model of the Shutter 38

Photometric Model of the Shutter 45

VI Results and Conclusions 55

Characteristics of this shutter 55

Uses for the Model 55

Improvements to the Model 56

Conclusion 57

VII References 59

VIII Appendix 1 62

IX Appendix 2 63

X Appendix 3 64

Table of Figures

Typical exposure program for automatic exposure 2

Mechanical shutter timing mechanism 3

Highly permeable material in a uniform field 9

B-H curve for steel 10

Magnetizing curve for steel and its hysteresis loop 11

B-H curve for permanent magnet 12

Region of field with different boundaries 14

Film characteristic curve 25

Real versus ideal shutter trace 30

Complete shutter assembly 32

3D view of the magnets, coils and lower fluxplate 33

2D approximation of the electromagnetics 33

Finite element mesh for one magnet position 35

B field for one magnet position 35

Energy of field vs magnet position 37

Magnetic force vs magnet position 38

Geometry of rotor and one shutter blade 40

Equivalent linkage for rotor and one shutter blade 40

Equivalent inertia of blade 42

Rotor angle versus time trace 45

CAD layouts for aperture area 46

Aperture area versus rotor angle 46

Aperture area and rotor angle versus time trace 47

Position curves for three drive times 50

Corresponding aperture curves 50

Area under the aperture curve vs drive time for 3 springs 51

Predicted exposure versus drive time 54
Predicted exposure program 54
MathCAD calculation of maximum opening 62
MathCAD calculation of inertia 63

List of Tables

Symbols and Units 9
Magnetic Model Data 34
Finite Element Results 37
Blade Inertia Data 39
Results from Shutter Simulations 53

List of Symbols

Magnetic Symbols

$\mathbf{H}$	Magnetic field intensity
$\mathbf{J}$, $J(x,y)$	Current density
$\mathbf{B}$, (B_{rx}, B_{ry})	Magnetic flux density
∇	Differential vector operator
$\mathbf{B}_r$	Remnant flux density
μ_0	Permeability of free space
μ_r	Relative permeability
μ	Absolute permeability
ν	Reluctivity
$\mathbf{H}_c$	Coercive force
$\mathbf{A}$, $A(x,y)$	Magnetic vector potential
Ω	General region
Γ	Boundary of region
α	Shape function
$I(A)$	Quadratic energy functional
K_{ij}^e	Magnetic finite element stiffness matrix
F_i^e	Magnetic finite element load vector
E	Energy
F_x	Force, x component

Exposure Symbols

I	Intensity
t	Time
E	Exposure
t	Shutter speed
TV	Time value
A	F-number
AV	Aperture value
EV	Exposure value
B	Brightness
BV	Brightness value
SV	Film speed value

Mechanical Symbols

x_R	Circumferential displacement of the magnet
R_{mag}	Radial distance to magnet center
θ	Rotor angle
I	Mass moment of inertia
C	Damping coefficient
K	Spring constant
T	Torque
I_{rotor}	Inertia of the rotor
R_m	Radial distance to moving pin
(A_x, A_y)	Location of the moving pin from the fixed pin

R_B	Distance from blade centroid to moving pin
R_f	Radial distance to fixed pin
ω	Rotor angular velocity
u	Distance between fixed pin and moving pin
ϕ	Angle from fixed pin to moving pin
v	Speed of the blade centroid
M	Mass of the blade
I_B	Blade inertia
I_{eq}	Equivalent blade inertia
I^*	Equivalent system inertia
e	Coefficient of restitution

ACSL Symbols

A	Aperture area
SUMA	Area under the aperture area vs time curve
AMAX	Maximum aperture area
X	Rotor angle
T	Time
OT	Drive time
SK	Spring constant
TT	Total shutter open time

I Introduction

Photographic cameras have a shutter and an aperture to control the amount of light received by the film. Traditionally, in Single Lens Reflex (SLR) cameras, the setting of the aperture is done by a mechanism separate from the shutter. The shutter is powered by a spring-driven mechanism that needs to be recharged by another energy source: the user's thumb in manual film advance cameras, or a small motor in motorized film advance cameras. Since a gear train is required to advance the film and recharge the shutter, the gears and linkages required to accomplish both tasks are complex.

Manual exposure cameras required the user to set the aperture and shutter speed prior to releasing the shutter. As cameras became more automated, automatic exposure became a required feature. To provide automatic exposure, the film speed and light level must be input to the camera and the camera logic must select an aperture and shutter speed to give a correct exposure. Since there are a large set of aperture and shutter speed combinations that provide a correct exposure, the camera logic must select one. The selection is made according to an exposure program as shown in Figure 1.

Automatic exposure cameras require additional mechanisms to automatically set the aperture prior to shutter release according to the exposure program. The mechanisms needed to meet all these requirements made for very complex, bulky and expensive cameras.

Some relief from the size and complexity of the SLR camera with a separate aperture mechanism and focal plane shutter was introduced when the two systems were combined into a leaf shutter. A leaf shutter provides both functions by operating at the aperture location of the lens and makes compact cameras possible. Most leaf shutters used in programmed exposure cameras have two or more blades that move to create a variable sized opening at the center of the lens. The first such devices were spring driven and required

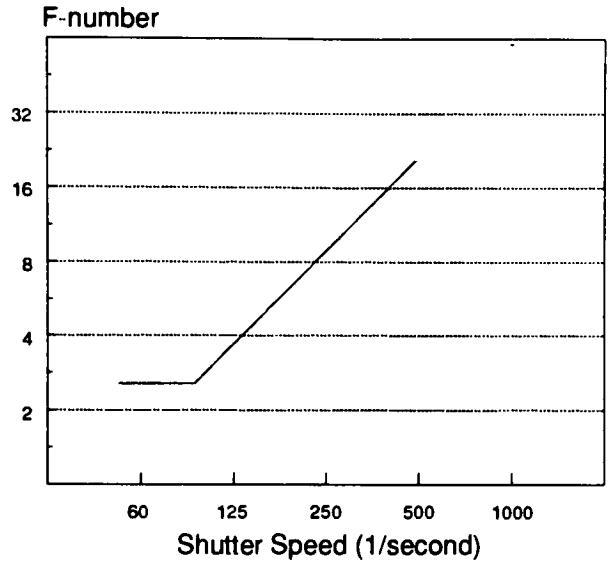

Figure 1. Typical exposure program for automatic exposure.

gears to transfer energy from the film advance system. In order to provide the programmed exposure in a mechanically driven system, a complex timing mechanism (Figure 2) is required in addition to the shutter and gear train.

Recently there has been much simplification in the mechanism needed to drive these programmed exposure leaf shutters. Electrical energy is easily delivered on two thin wires, which replace the bulky and complex gear train that was required to deliver mechanical energy to the shutter. Control of the shutter timing is now done with electronic circuits which replace a bulky and complex mechanical timing mechanism. This has resulted in simpler, smaller and lower priced cameras.

The electrical energy is used to generate magnetic flux which applies a force to permanent magnets and causes shutter motion. The force generated by a spring is well understood and prediction of that force is fairly easy to accomplish for a given spring design. The force generated by a permanent magnet in a magnetic field is not as easy to predict. The theory and results of predicting magnetic forces are described in this investigation.

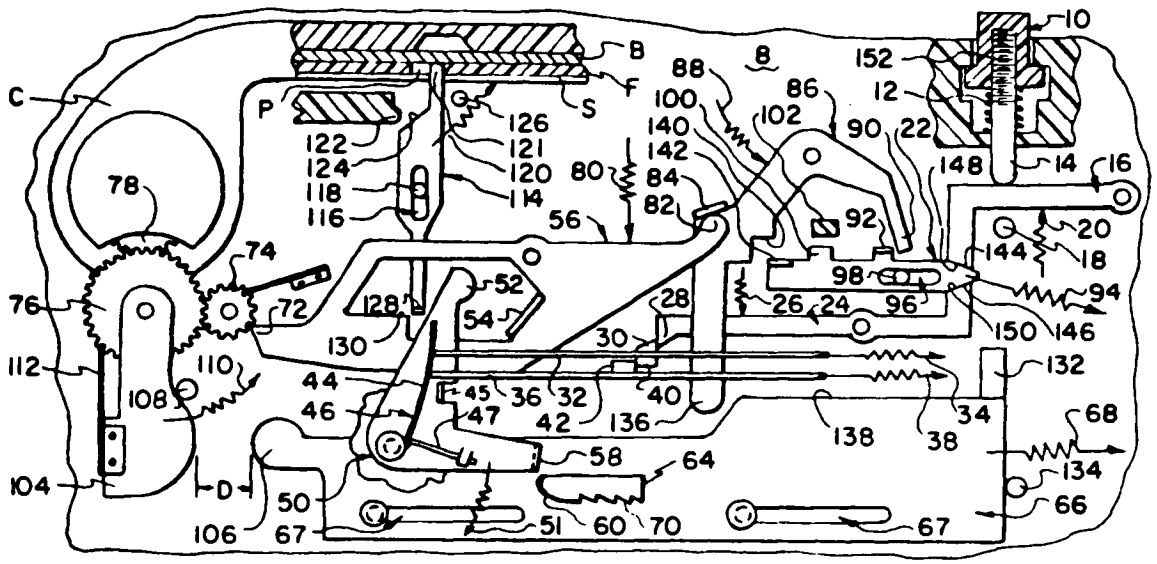

Figure 2. Mechanical shutter timing mechanism.

A shutter model is needed because magnetic forces are smaller than spring forces but rapid response time is required. A math model of the shutter provides a tool for optimizing the design to provide the performance required in the smallest amount of space. The math model would be used in conjunction with a prototype, however, optimization is faster and cheaper using a math model, compared to building multiple prototypes. Furthermore, insight may be gained from the math model that is not obvious from the prototype testing.

The shutter system is a complex device to model. In order to build a model of the shutter, the analysis is split into three models: the magnetic model, the mechanical model and the photometric model. The results of the magnetic model (forces) are used in the dynamic simulation of the mechanical model, and the results of the dynamic simulation (position-time) are used in the photometric model.

II Literature Review

In this section, the development of electromagnetic modeling using the finite element method will be reviewed, along with examples of dynamic simulations of other magnetic actuators.

Electromagnetic Field Solutions

One of the most widely cited papers in the literature was written by Silvester and Chari [1] in 1970. In their paper, Silvester and Chari presented a nonlinear energy functional from which was derived the basic partial differential equation governing the problem. This paper was the first in which the nonlinear effect of magnetic saturation of a core was solved numerically. The finite element mesh consisted of linear triangular elements and the problem formulated was a two dimensional boundary value problem with the magnetic vector potential **A** as the primary variable.

Brauer [2] draws an analogy between the governing nonlinear differential equations of magnetic fields and heat transfer to show how MSC/NASTRAN's heat transfer analysis capability may be used to solve linear magnetic field problems formulated in two dimensional rectangular cartesian coordinates. He also demonstrated that axisymmetric problems of heat transfer are not analogous to axisymmetric magnetic fields because of an extra term introduced due to **A** being a vector quantity. Brauer gives the nonlinear energy functional without proof and develops a finite element formulation based on it.

Guancial and DasGupta [3] have attempted to compare three-dimensional solutions with those of two-dimensional solutions using the finite element method to solve for the magnetic vector potential. They are among the few authors to explicitly state that their equa-

tions do not consider permanent magnets. The geometry for which they obtain solutions consists only of rectangular prisms. Some other authors have concluded that the magnetic vector potential is unsuitable for three-dimensional problems because there are three variables at each node instead of one. They have developed alternatives to the magnetic vector potential that result in only one variable at each node. These methods are known as the total scalar potential [4], the reduced scalar potential [5], hybrid methods or more recently, the new scalar potential [6].

A good summary text for these papers is the book by Silvester and Ferrari [7].

Field Solutions including Permanent Magnets

Few of the early papers exploring the use of finite elements in the solution of magnetic field problems are concerned with permanent magnets as a source of flux. They are devoted almost entirely to current-carrying conductors as the source of flux. The first paper to include permanent magnets was by Reichert [8]. He derived finite difference equations for a two dimensional problem based on a rectangular grid.

When using finite element software that does not have the capability to include permanent magnets directly, one of the techniques of modeling permanent magnets is to replace the magnet with an equivalent current sheet [9]. As modern hard permanent magnet materials were developed that had essentially linear characteristics, simple models of this material were added to the finite element computer codes that had the capabilities to solve magnetostatic problems [10].

Magnetic Force Calculation

The energy method provides one of the most straight-forward techniques of calculating magnetic force. Marinescu and Marinescu [11] investigate the computation of torque by both the Maxwell stress tensor and the gradient of magnetic energy with respect to position. A loss of accuracy occurs in the force calculation by the energy method due to the differencing of nearly identical energies. Accuracy of the force calculation in the Maxwell stress method depends on choosing a suitable path for surface integration. The advantage of the energy method is that the energy may be calculated from the result of the field solution.

A technique exists for determining magnetic force by applying virtual work to each finite element [12], rather than using finite displacements of the bodies as in the energy method. However, the virtual work equations for solving for magnetic force must be written into the finite element code that solves the magnetostatic problem.

Dynamics of Mechanisms

Mechanically, the shutter is a mechanism constrained to one degree of freedom that has several parts moving at varying relative speeds. Since there are several speeds in the system at any instant, one part is chosen to represent the system speed. The method used to simplify the dynamics of the multibody system to an equivalent single degree of freedom system is to equate kinetic energies. The inertia of each body is varied to equate its kinetic energy calculated at the system speed with its original kinetic energy. This method is outlined in Appendix 6A of a book by Tesar and Matthew [13].

Dynamic Performance of Electromechanical Systems

Electromagnetics also plays a role in shutter dynamics. There are a few examples of electromechanical dynamics in the literature. Elliott [14] obtains position-time data for an electromechanical relay by use of the circuit model of the magnetics.

Ancelle, Coulomb and Morel [15] describe a CAD system for the design of electromagnets, which uses the finite element method to obtain the magnetic force and the circuit inductance for a set of air-gaps. This data is used in the integration of the coupled equations of motion to provide a dynamic simulation.

Howe and Low's paper [16] deals with the dynamic performance of rotary and linear stepper motors. The Maxwell stress tensor is used to calculate the static forces and torques generated by the magnets with the coil current both on and off at a set of rotor positions. An unspecified dynamic simulation solves the given equations of motion and position-time curves are plotted. The effects of driving under constant current as well as by capacitor discharge are analyzed.

III Electromagnetic Field Theory

Maxwell's Equations - Magnetostatics

Electromagnetic fields are governed by Maxwell's equations. The magnetostatic assumption requires that the velocity of the moving parts has a negligible effect on the field. The three-dimensional magnetostatic equations in differential form are written in SI units as

$$\nabla \times \mathbf{H} = \mathbf{J} \tag{1}$$

$$\nabla \cdot \mathbf{B} = 0 \tag{2}$$

$$\mathbf{B} = \mathbf{B}_r + \mu \mathbf{H} \tag{3}$$

where $\mu = \mu_r \mu_0$

The relevant units are shown in Table 1. Equation (3) is known as the constitutive equation since it relates the field quantities in a given material. The remnant flux density, $\mathbf{B}_r$, exists only inside permanent magnetic materials and can be assumed constant for hard magnetic materials. Materials that are not magnetized have $\mathbf{B}_r = 0$. Thus the flux density, **B**, which unmagnetized materials carry in the presence of a magnetic field of intensity, **H**, depends on its permeability, μ. Thus permeability is a measure of the ease with which a material will carry magnetic flux. The presence of a highly permeable material in a magnetic field has the effect of creating a path of least resistance to carry the flux. The lines of flux tend to bend and become very concentrated in the material as shown in Figure 3.

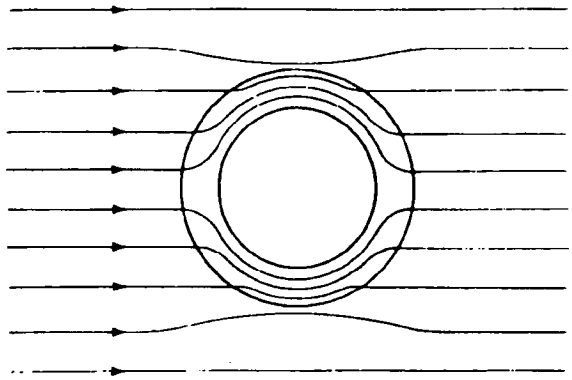

Figure 3. Highly permeable material in a uniform field, from Cullity [17].

Table 1. Units and Symbols.

Symbol	Name	SI Units
H	Magnetic field intensity	A/m
J	Current density	A/m^2
B	Magnetic flux density	Wb/m^2
$\mathbf{B}_r$	Remnant flux density	Wb/m^2
μ_0	Permeability of free space	$4\pi \times 10^{-7}$ Wb/(Am)
μ_r	Relative permeability	Dimensionless
μ	Absolute permeability	$\mu = \mu_r \mu_0$
ν	Reluctivity	$\nu = 1/\mu$

The SI units are ampere (A), meter (m), and weber (Wb). A weber is defined as the magnetic flux which, linking a circuit of one turn, produces in it an electromotive force of 1 volt as it is reduced to zero at a uniform rate in 1 second. This definition describes the Farady-Lenz law given by

$$V = N\frac{d\Phi}{dt} \tag{4}$$

where Φ is the flux that passes through N turns of a coil. English units are still commonly used in magnetics. The units for **B** are gauss (G) and the units for **H** are oersteds (Oe), and they are numerically equal since permeability is dimensionless in the English system. Cullity [17] has a good discussion on the history of units in magnetics.

Magnetic Materials

Steel

Steel is a very permeable material. Compared with air, which has a relative permeability of about 1, steel has a relative permeability of about 1,000. Steel is a nonlinear material since $\mu = \mu(\mathbf{B})$ and exhibits saturation at high field intensities. Below saturation, steel can be assumed to be a linear material, so μ is constant. The magnetic flux in the steel is assumed to follow the curve without hysteresis, so no remnant magnetization is introduced and $\mathbf{B}_r = 0$ in the steel (Figure 4).

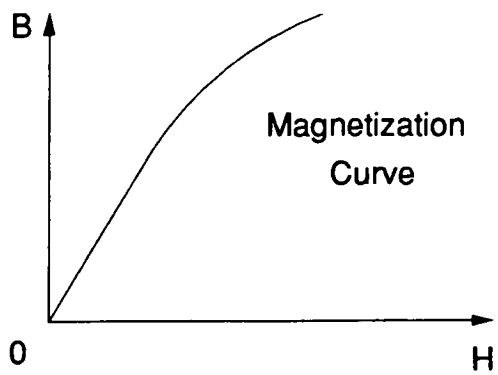

Figure 4. B-H curve for steel. The slope of the curve is μ.

If the applied field continues to increase, the steel will become permanently magnetized and on removal of the applied field, the steel will follow its demagnetization curve down

to its remnant magnetic state, $\mathbf{B}_r$ (Figure 5). Now if the applied field is reversed in direction, the flux density in the material will continue to follow the demagnetization curve down until the applied field exactly cancels the permanent flux at the point called the coercive force, $\mathbf{H}_c$. A continual increase of the applied field in the reverse direction will permanently magnetize the steel in the reverse direction. Another reversal of the applied field back to the original direction will close the hysteresis loop. Steel is magnetically soft because the magnitude of the applied field required to magnetize it is small compared to magnetically hard materials.

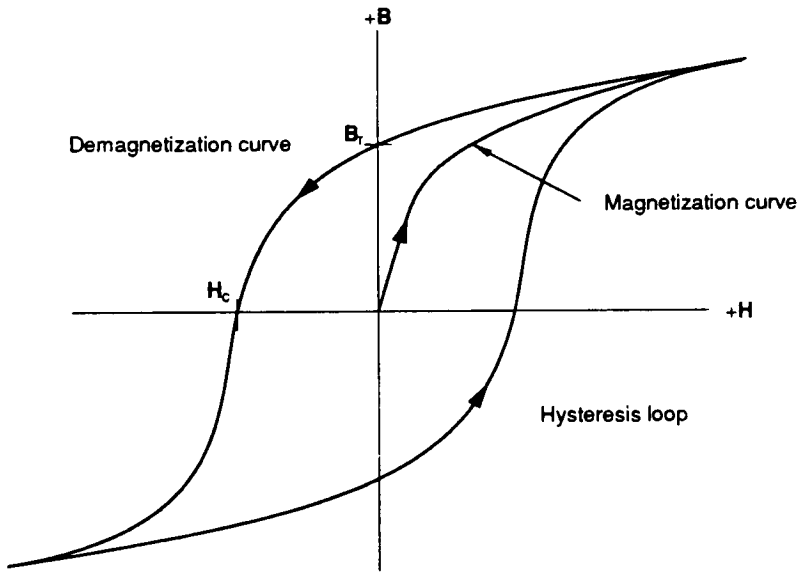

Figure 5. Magnetizing curve for steel and its hysteresis loop.

When permanent magnets are used in a device, the flux that they generate is used to do work and must not change. Therefore they are not placed in applied fields strong enough to reverse the direction of permanent magnetization. The part of the hysteresis loop that is used in a device is in the second quadrant of the demagnetization curve of Figure 5.

Permanent Magnets

Hard permanent magnetic materials have a linear B-H curve (Figure 6) and have a relative permeability about the same as air. That means that an unmagnetized bar of hard magnetic material is no better than air at carrying flux and that there would be no concentration of flux in a bar of hard magnetic material in a magnetic field. Once magnetized, hard magnetic materials have the property of remnant magnetization which gives $\mathbf{B}_r$ as constant inside the material. That means that there will be a flux at the surface of the material without the presence of an applied magnetic field.

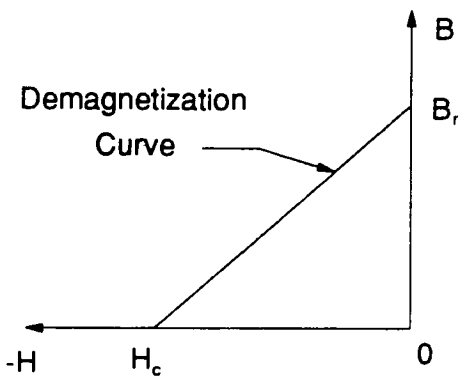

Figure 6. B-H curve for permanent magnet.

The magnetic field intensity, **H**, inside the permanent magnet has two components, the applied field and the demagnetization (demag) field ($\mathbf{H} = \mathbf{H}_a + \mathbf{H}_d$). For isotropic materials, the three vectors inside the material **B**, $\mathbf{B}_r$, and $\mathbf{H}_d$ are all collinear and the demag field is always in the direction opposite that of $\mathbf{B}_r$. While the magnitude of remnant flux density is a material property, the magnitude of the demag field is a function of the magnet geometry. Long thin bar magnets have a small demag field while thin "coin-like" magnets, magnetized perpendicular to the coin face, have extremely high demag fields. However, the demag field can never entirely cancel the remnant flux density. Therefore, a permanent magnet in a bar configuration will deliver much more flux than a magnet in a coin configuration.

Two Dimensional Magnetic Vector Potential

An additional quantity, the magnetic vector potential, **A**, is introduced and is defined by

$$\nabla \times \mathbf{A} = \mathbf{B} \tag{5}$$

which automatically satisfies the zero divergence of **B** required by Equation (2). Substitution of Equation (5) into the constitutive equation gives

$$\nu \nabla \times \mathbf{A} - \nu \mathbf{B}_r = \mathbf{H} \tag{6}$$

where $\nu = 1/\mu$.

Substituting this into the first of Maxwell's equations results in

$$\nabla \times \nu \nabla \times \mathbf{A} - \nabla \times \nu \mathbf{B}_r - \mathbf{J} = 0 \quad \text{in the region } \Omega. \tag{7}$$

General Equation for the Field.

Now consider some simplifications to the general case. The present work is concerned with linear isotropic materials, so ν reduces from a tensor and a function of **B** to a scalar constant. Another simplification that will be made is to make a two dimensional approximation of the geometry. In the 2D linear case the vectors reduce to

$$\mathbf{A} = A(x, y)\hat{k} \tag{8}$$
$$\mathbf{J} = J(x, y)\hat{k}$$

With ν constant, apply the identity

$$\nabla \times \nabla \times \mathbf{A} = \nabla(\nabla \cdot \mathbf{A}) - \nabla^2 \mathbf{A} \tag{9}$$

then use the Coulomb gauge described in Lowther and Silvester [18] of $\nabla \cdot \mathbf{A} = 0$ to give

$$\nabla \times \nabla \times \mathbf{A} = -\nabla^2 A(x,y)\hat{k}$$

and apply the identity

$$\nabla \times \nu \mathbf{B}_r = \left(\frac{\partial \nu B_{ry}}{\partial x} - \frac{\partial \nu B_{rx}}{\partial y} \right) \hat{k} \tag{10}$$

to obtain a scalar equation from the vector equation

$$\nu \nabla^2 A + \left(\frac{\partial \nu B_{ry}}{\partial x} - \frac{\partial \nu B_{rx}}{\partial y} \right) + J = 0 \quad \text{in} \quad \Omega \tag{11}$$

2D Linear Field Equation

where $B_{rx}(x,y)$, $B_{ry}(x,y)$, and $J(x,y)$ are known functions of position.

In variational terms, this is the strong form of the problem because it must be satisfied at every point within the region. The region is shown in Figure 7 with boundaries Γ_0, Γ_1, and Γ_2 which are defined below.

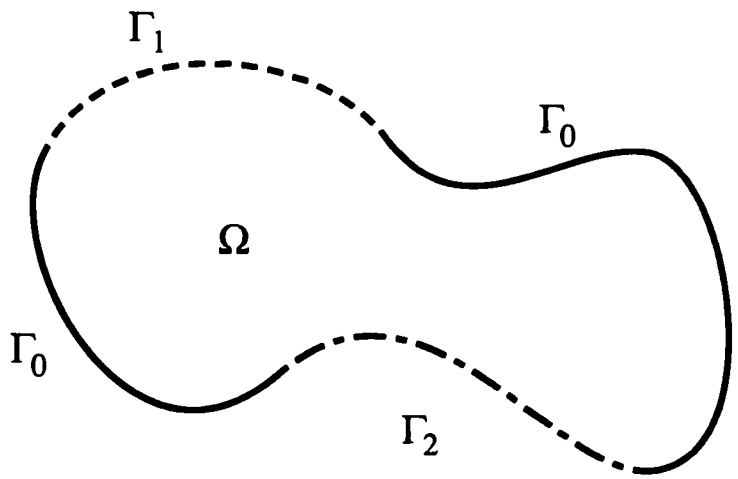

Figure 7. Region of field with different boundaries.

Solution of the Vector Potential

A solution of the 2D linear field equation is required in order to obtain the field energy which will be used in the calculation of the magnetic force. A function $A(x,y)$ is sought which satisfies the above field equation over the region and satisfies the specified boundary conditions. Variational methods provide one way to solve partial differential equations [19]. To obtain the weak form of the problem, multiply Equation (11) by an admissible test function $\alpha(x, y)$ and integrate over the region. The test function must satisfy the homogeneous form of the essential boundary conditions (Dirichlet boundary conditions) and be sufficiently differentiable.

$$\int_{\Omega} \alpha \left[\nu \nabla^2 A + \left(\frac{\partial \nu B_{ry}}{\partial x} - \frac{\partial \nu B_{rx}}{\partial y} \right) + J \right] dxdy = 0 \tag{12}$$

Apply the following identity to the first term in order to integrate by parts,

$$\int_{\Omega} (\nabla^2 f) g \, dxdy = -\int_{\Omega} \nabla f \cdot \nabla g \, dxdy + \oint_{\Gamma} \frac{\partial f}{\partial n} g \, ds. \tag{13}$$

To the second term, componentwise, apply the identities

$$g \frac{\partial F_y}{\partial x} = \frac{\partial}{\partial x}(g F_y) - F_y \frac{\partial g}{\partial x} \tag{14}$$

and

$$\int_{\Omega} \frac{\partial}{\partial x}(g F_y) dxdy = \oint_{\Gamma} g F_y n_x ds.$$

Thus Equation (12) is rewritten as

$$0 = -\int_{\Omega} \nu \nabla \alpha \cdot \nabla A dx dy + \int_{\Omega} J \alpha dx dy \tag{15}$$
$$+ \int_{\Omega} \left(\nu B_{rx} \frac{\partial \alpha}{\partial y} - \nu B_{ry} \frac{\partial \alpha}{\partial x} \right) dx dy$$
$$+ \oint_{\Gamma} (\alpha \nu B_{ry} n_x - \alpha \nu B_{rx} n_y) ds + \oint_{\Gamma} \nu \frac{\partial A}{\partial n} \alpha ds$$

Specification of A on a segment Γ_0 of the boundary constitutes an Essential (or Dirichlet) Boundary Condition (EBC). In the magnetic model to follow, A is set to zero on the boundary. Specification of

$$\nu \frac{\partial A}{\partial n} = \hat{q}_n \quad \text{on} \quad \Gamma_1 \tag{16}$$

or specification of

$$\nu B_{ry} n_x - \nu B_{rx} n_y = f_n \quad \text{on} \quad \Gamma_2 \tag{17}$$

constitutes a Natural (or Neumann) Boundary Condition (NBC). Equation (17) is the boundary condition applied when there is magnetized material on the boundary and it specifies the magnitude and direction of the permanent field at the boundary. Where the specification of A on the boundary is not made, the boundary term vanishes because at those points $\alpha = 0$.

Thus, Equation (15) becomes

$$0 = -\int_{\Omega} \nu \nabla \alpha \cdot \nabla A dx dy + \int_{\Omega} J \alpha dx dy + \int_{\Omega} \left(\nu B_{rx} \frac{\partial \alpha}{\partial y} - \nu B_{ry} \frac{\partial \alpha}{\partial x} \right) dx dy + \oint_{\Gamma_1} \hat{q}_n \alpha ds + \oint_{\Gamma_2} f_n \alpha ds \tag{18}$$

This is the weak form of the problem. It is weak in the sense that there may be local departures from the strong form as long as it is satisfied "on the average." The weak form contains a bilinear and linear term given respectively by

$$B(\alpha, A) = \int_{\Omega} \nu \nabla \alpha \cdot \nabla A dx dy \tag{19}$$

$$l(\alpha) = \int_{\Omega} \left(J\alpha + \nu B_{rx} \frac{\partial \alpha}{\partial y} - \nu B_{ry} \frac{\partial \alpha}{\partial x} \right) dx dy + \oint_{\Gamma_1} \hat{q}_n \alpha ds + \oint_{\Gamma_2} f_n \alpha ds$$

Since B is bilinear and symmetric and l is linear, the quadratic functional associated with the variational form above is obtained from

$$I(A) = \frac{1}{2} B(A,A) - l(A) \tag{20}$$

along with any specified essential boundary conditions.

Therefore the appropriate quadratic functional is given by

$$I(\mathrm{A}) = \frac{1}{2}\int_{\Omega} \nu \nabla \mathrm{A} \cdot \nabla \mathrm{A} dxdy - \int_{\Omega} \mathrm{J}\mathrm{A} dxdy - \int_{\Omega}\left(\nu \mathrm{B}_{r_x}\frac{\partial \mathrm{A}}{\partial y} - \nu \mathrm{B}_{r_y}\frac{\partial \mathrm{A}}{\partial x}\right)dxdy - \oint_{\Gamma_1} \hat{q}_n \mathrm{A} ds - \oint_{\Gamma_2} f_n \mathrm{A} ds \tag{21}$$

However,

$$\mathbf{B} = \frac{\partial \mathrm{A}}{\partial y}\hat{i} - \frac{\partial \mathrm{A}}{\partial x}\hat{j} = \mathrm{B}_x\hat{i} + \mathrm{B}_y\hat{j} \tag{22}$$

Substitution of Equation (22) into the third term of Equation (21) results in

$$I(\mathrm{A}) = \int_{\Omega}\left[\frac{1}{2}\nu(\nabla \mathrm{A})^2 - \mathrm{J}\mathrm{A} - \nu \mathbf{B}_r \cdot \mathbf{B}\right]dxdy - \oint_{\Gamma_1} \hat{q}_n \mathrm{A} ds - \oint_{\Gamma_2} f_n \mathrm{A} ds \tag{23}$$

Quadratic Energy Functional

The exact minimization of the energy functional yields a function $A(x,y)$ which is the solution of the original differential equation. The value of the energy functional evaluated at the minimizing function is the associated field energy.

Approximate Solution

The exact solution A(x,y) which minimizes the functional can be expressed as

$$A(x,y) = \alpha_0(x,y) + \sum_{j=1}^{\infty} c_j \alpha_j(x,y) \tag{24}$$

where α_0 satisfies the EBC's, the α_j are the known fixed basis or shape functions and the c_j are the unknown coefficients which describe the exact solution. The difficulty with this form of the exact solution is that the basis functions must "fit" the problem region. Further, there are infinitely many unknown coefficients.

Discretization

The first step in obtaining an approximate solution is to discretize the problem into "finite elements" which individually have a simpler geometry than the overall region. A common discretization consists of triangular elements. The basis functions now need only satisfy the boundary conditions on each element's (simple) boundary. The global solution is then approximated in a piecewise fashion, however there are still an infinite number of unknowns because A in Equation (24) is described by an infinite series.

Finite Number of Unknowns

The second step in the approximate solution is to reduce the number of basis functions and the corresponding unknown coefficients. This is done by allowing the functional to be minimized only by polynomial functions whose coefficients are the unknown variables. Combining these ideas gives the form of the approximate solution over one of the finite elements as

$$A(x,y) = \sum_{j=1}^{n} A_j \alpha_j(x,y) \tag{25}$$

Here A_j is the value of A at the nodes of the element and $\alpha_j(x,y)$ is the interpolating basis function over that element. A typical basis function on a second order element takes the form

$$\alpha(x,y) = c_0 + c_1 x + c_2 y + c_3 x^2 + c_4 xy + c_5 y^2. \tag{26}$$

Substituting Equation (26) into the weak form given by Equation (18) and letting the test function be α_i yields

$$0 = \sum_{j=1}^{n} \left\{ -\int_{\Omega^e} \nu \nabla \alpha_i \cdot \nabla \alpha_j dxdy \right\} A_j + \int_{\Omega^e} J\alpha_i dxdy + \int_{\Omega^e} \left(\nu B_{rx} \frac{\partial \alpha_i}{\partial y} - \nu B_{ry} \frac{\partial \alpha_i}{\partial x} \right) dxdy + \oint_{\Gamma^e} \hat{q}_n \alpha_i ds \qquad i = 1, 2, \ldots, n \tag{27}$$

where the term containing f_n has been dropped since in this case the boundary will not cut the permanent magnet (Figure 13). The above equation may be written in compact form as

$$\sum_{j=1}^{n} K_{ij}^e A_j^e = F_i^e \tag{28}$$

where $$K_{ij}^e = \int_{\Omega^e} [\nu \nabla \alpha_i \cdot \nabla \alpha_j] dxdy$$

and $$F_i^e = \int_{\Omega^e} \left[J\alpha_i + \left(\nu B_{rx} \frac{\partial \alpha_i}{\partial y} - \nu B_{ry} \frac{\partial \alpha_i}{\partial x} \right) \right] dxdy + \oint_{\Gamma^e} \hat{q}_n \alpha_i ds.$$

Finite Element Model of the Problem

K^e is the element stiffness matrix and F^e is the element forcing vector. As K^e and F^e are calculated for each element, they are assembled into a global stiffness matrix and a global forcing vector. Element connectivity is used to constrain nodes common to more than one element to have the same nodal values. Thus a large system of (in this case) linear equations is derived which when solved gives the value of the unknown A at every node point. By virtue of the interpolating shape functions, A is also known at every point in the region.

Field Energy

The field solution obtained, the energy of the field must be calculated so that the magnetic force can be derived. Since the force is calculated as the spatial gradient of the field energy, the force will be the same regardless of any included additive constant in the field energy.

An energy integral that will result in the appropriate force is

$$E = \frac{1}{2}\int_{\Omega} \mu H^2 dxdy - \int_{\Omega} JA dxdy \tag{29}$$

Energy Integral

where the only boundary conditions specified are essential boundary conditions or homogeneous Neumann boundary conditions ($\hat{q}_n = 0$).

Recall that the value of the energy functional, when minimized, is the associated magnetic field energy. It will be shown below that the energy integral of Equation (29) is identical to the energy functional of Equation (23) plus an additive constant. This is

important because Equation (23) has been derived from Maxwell's equations while Equation (29) will be used to calculate the field energy since the terms in Equation (29) can be easily computed in the magnetostatic finite element software.

Since

$$H^2 = \mathbf{H} \cdot \mathbf{H}$$

and

$$\mathbf{H} = \nu(\nabla \times \mathbf{A}) - \nu \mathbf{B}_r$$

substitution in the energy integral of Equation (29) yields

$$\begin{aligned} E &= \frac{1}{2}\int_{\Omega} \mu[\nu(\nabla \times \mathbf{A}) - \nu \mathbf{B}_r] \cdot [\nu(\nabla \times \mathbf{A}) - \nu \mathbf{B}_r] dxdy - \int_{\Omega} \mathrm{J}\mathrm{A} dxdy \\ &= \frac{1}{2}\int_{\Omega} \nu[(\nabla \times \mathbf{A})^2 - 2\mathbf{B}_r \cdot \mathbf{B} + \mathbf{B}_r^2] dxdy - \int_{\Omega} \mathrm{J}\mathrm{A} dxdy \\ &= \int_{\Omega} \left[\frac{1}{2}\nu(\nabla \mathrm{A})^2 - \nu \mathbf{B}_r \cdot \mathbf{B} - \mathrm{J}\mathrm{A} \right] dxdy + \frac{1}{2}\nu \int_{\Omega} \mathrm{B}_r^2 dxdy \end{aligned} \tag{30}$$

Finally,

$$E = I(\mathrm{A}) + \frac{1}{2}\nu \int_{\Omega} \mathrm{B}_r^2 dxdy. \tag{31}$$

Under the assumptions established earlier, the last term is constant so that the force calculated from the gradient of this energy integral will be identical to the force calculated from the gradient of the energy functional.

Magnetic Force Calculation

The magnetic force generated by the set of fields needs to be calculated so that the dynamics of the problem can be formulated.

A well known physical principle called virtual work states that for conservative systems, force is the gradient of stored energy. The finite element method is implemented to approximate the energy E of an electromagnetic field. The gradient of the energy of the field solution gives the force at that configuration as

$$F_x = \frac{\partial E}{\partial x} \tag{32}$$

For constant current input, this force will be a function of displacement only. A second order finite difference method will be described in the magnetic modeling section to obtain the numerical gradient of the energy.

IV Exposure Calculations

The purpose of a shutter is to expose film. Exposure is defined as the amount of light hitting the film:

$$E = I \times t \tag{33}$$

where I is the intensity of the exposing light and t is the time in seconds. Film is a photosensitive emulsion that responds to light in a geometric way. If the amount of exposing light falling on the film increases, the transmittance, T, of the printing light through the developed negative is reduced depending on the slope of the film's DlogE characteristic curve (Figure 8). This is due to a change in film density (how dark the negative looks), where density is defined as

$$D = \log(1/T). \tag{34}$$

If the film is in the linear portion of its curve, the change in density is proportional to the change in log exposure. Film will behave linearly over a large but limited range of exposures. A typical DlogE characteristic curve is shown in Figure 8.

Measurements of exposure are made in units of stops, where an increase of one stop represents a doubling of exposure. There are four factors that relate to exposure: shutter speed, aperture, film speed, and brightness.

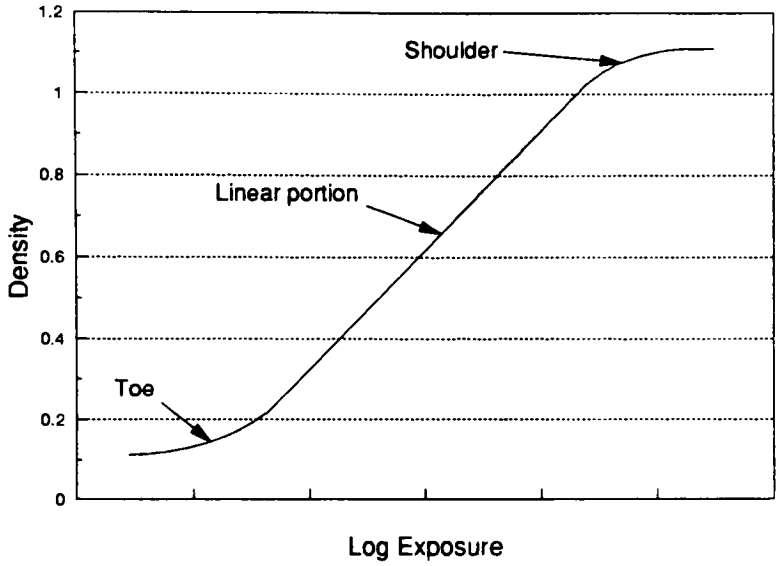

Figure 8. Film characteristic curve.

Shutter Speed

Shutter speed, t, is a misnomer. What is meant is shutter time measured in seconds. SLR cameras commonly have shutter speed markings on the controls of 1/60, 1/125, and 1/250. It is noted that these settings differ by roughly a factor of two. Shutter speed is mapped to a variable called Time Value or TV which has the units of stops. The mapping is

$$\mathrm{TV} = -\frac{\log(t)}{\log(2)} \tag{35}$$

where the rule for calculation of logarithms base 2 has been applied. The inverse mapping is

$$t = 2^{-\mathrm{TV}} \tag{36}$$

which explains how the markings on the camera came about. They are the approximate values corresponding to TV = 6, 7, and 8.

Note that when TV increases by one, the shutter time is decreased by a factor of two and the film is exposed for half as long.

Aperture

Aperture has many meanings in cameras. An aperture is the opening through which the light passes to get to the film. If the opening is approximately circular then its diameter, d, is a measure of the intensity of light hitting the film. If the opening is non-circular, then the term effective aperture is used and the diameter of the circle of equal area is used. However because the aperture is a feature of the lens, the intensity of light also depends on a characteristic of the lens called the focal length, f. The variable that defines the intensity of light that may pass through a lens is called the f-number, A, and is defined as

$$A = \frac{f}{d} \tag{37}$$

The same light intensity will pass through a diameter twice as large if the second lens has twice the focal length of the first lens. The markings commonly found on the side of an SLR lens are 5.6, 8, and 11. F-number is mapped to a variable called Aperture Value, AV, which has the units of stops.

$$AV = \frac{2\log(A)}{\log(2)} \tag{38}$$

The factor two that appears in the above expression is explained because f-number is defined with a diameter. When the f-number doubles, the diameter is halved and the area decreases by a factor of four, so the light intensity changes by a factor of four or 2 stops.

The inverse relation is

$$A = 2^{AV/2} \tag{39}$$

so the numbers on the side of the lens correspond to AV of 5, 6, and 7.
Note that when the AV increases by one, the f-number increases by a factor of $\sqrt{2}$, and the film gets half the intensity of light since the diameter is reduced.

Exposure Value

What happens if the aperture is increased by one stop while the shutter speed is decreased by one stop? The intensity of the light hitting the film is halved while the time that light is allowed to hit the film is doubled. The response of the film (the exposure) doesn't change. That result is captured in a variable called Exposure Value or EV which also has the units of stops.

$$EV = AV + TV \tag{40}$$

Exposure is a combination of intensity of light and duration. What is the correct exposure for a photograph? That depends on the film being used and the brightness of the scene. A correct exposure occurs when the brightness range in the scene is captured in the middle portion of the film density range.

Brightness

Brightness, *B*, is measured in footlamberts (fL). The variable that has the units of stops is called the Brightness Value or BV.

$$\mathrm{BV} = \frac{\log(B)}{\log(2)} \tag{41}$$

Daylight covers a wide range of brightness. The brightest scene is sun on snow and may be 2000 ft-L while scenes at dusk or in deep shade may be around 32 ft-L which is a range of six stops. A very dark scene is beyond the capability of common cameras and films to capture without the addition of the light from a flash. For a given film, the exposure has to be adjusted as the brightness changes.

Film Speed

Slow film needs more exposure to obtain densities in the middle of its response curve. Fast film needs less exposure, since it is more sensitive to light. Film speeds are given as ISO 100, 200, or 400, for example. The variable that has the units of stops is called Speed Value or SV.

$$\mathrm{SV} = \frac{\log(\mathrm{S/K})}{\log(2)} \tag{42}$$

K is known as the system constant and is an empirically determined constant usually close to 4.

Exposure Adjustment

If a camera is to be adjusted to obtain the correct exposure for different brightness levels, the film speed must enter into that calculation. A correct exposure can be made of a scene with twice the brightness by using a film half as sensitive to light, or half the ISO film speed. That relationship is given by

$$EV = BV + SV \tag{43}$$

Therefore all the parameters are related by

$$AV + TV = EV = BV + SV \tag{44}$$

If a camera is to obtain a correct exposure over the daylight range using a variety of films then the number of stops of exposure adjustment required increases to eight or more stops.

Shutter Characteristics

When a shutter is characterized, the quantities of interest are:

- Total time the shutter is open
- Maximum aperture achieved
- Exposure or area under the light trace vs time curve.

A shutter is tested by placing it between a light source and a photocell connected to an oscilloscope. The oscilloscope then traces the photocell response over time. The area under the curve is a measure of the exposure that a particular shutter delivers.

An ideal shutter would open instantaneously to the aperture set and remain there until the time set for the shutter speed had elapsed then instantaneously close. In such an ideal case the shutter speed would be the total time that the shutter was open and the entire exposure would have been made at a single aperture. The exposure would be related to the area under the curve calculated by the product of the shutter speed and the intensity allowed by the aperture. On a geometric scale, the Exposure Value would be the sum of the Time Value and the Aperture Value.

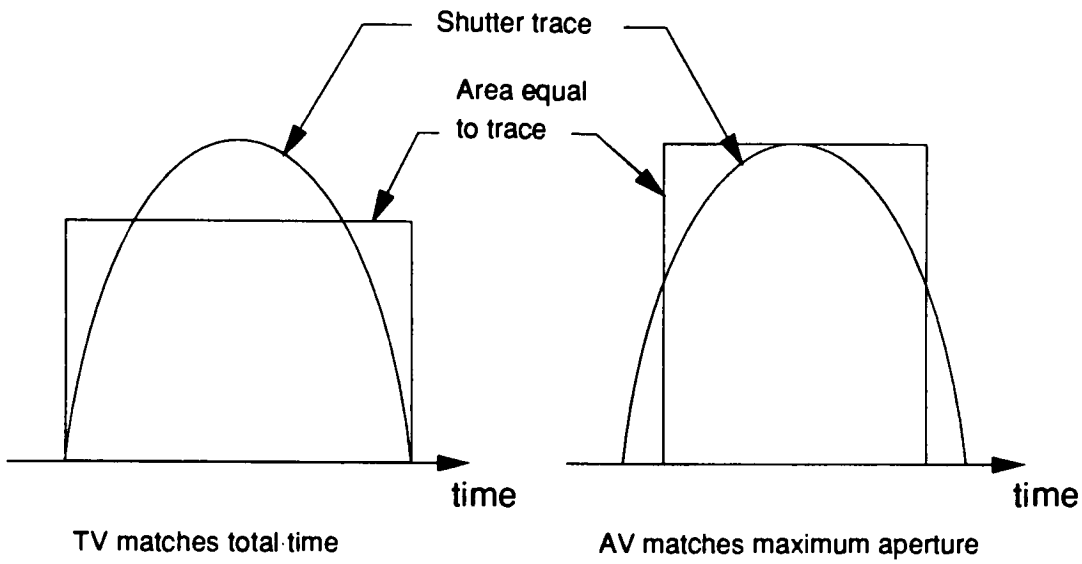

Figure 9. Real versus ideal shutter traces.

A real shutter does not open instantaneously and so the above definitions get somewhat ambiguous. The area under the curve is well defined and therefore, so is the exposure value. But when it comes to breaking EV down into two components for aperture and shutter speed, two possible definitions are shown in Figure 9. The definition adopted here is that the maximum aperture attained is used to calculate AV and the TV is then defined as

$$TV = EV - AV \tag{45}$$

However because this definition results in exposure times shorter than the actual time that the shutter is open, an additional measure will be taken, namely the total time that the shutter is open. This is important for considerations such as camera shake and subject motion.

V Shutter Model

Shutter Description

This shutter is a leaf shutter that is built into or behind the taking lens of a camera. It consists of four moving parts: three identical blades and a rotor. The blades are thin and they stack up in the center to create different size apertures (Figure 21) from each of the blade edges depending on where the rotor has positioned them. The blades have a slot that interfaces with a fixed pin and a hole that interfaces with a pin on the rotor, and the blades are moved by the relative motion of these two pins. The rotor has permanent magnets fastened to it which, when current flows in the coil, provide the driving force to open the shutter. The rotor also has an extension spring that acts to close the shutter.

The stationary parts of the shutter include the coils that are directly under the magnets, and an upper and lower steel plate that serves to conduct the magnetic flux. The fixed pins pass through slots in the rotor to provide the relative motion with the pins on the rotor. The maximum aperture that the lens allows would be part of the stationary base which completes the assembly. A complete shutter is shown in Figure 10.

The electrical input to run the shutter is assumed to be a step function to a fixed current level in the coil to drive the shutter open. After a fixed duration, called the drive time, the current is turned off and the shutter is driven closed by the force of the extension spring.

The shutter system is a complex device to model. In order to build a model of the shutter, the analysis is split into three models: the magnetic model, the mechanical model and the

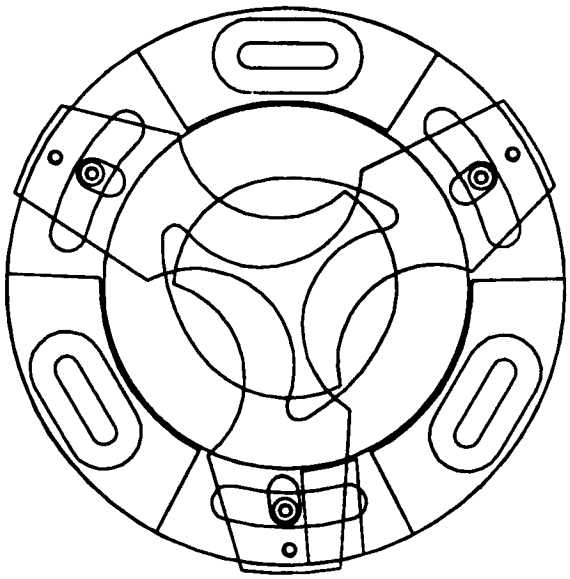

Figure 10. Complete shutter assembly.

photometric model. The results of the magnetic model (forces) are used in the dynamic simulation of the mechanical model, and the results of the dynamic simulation (position-time) are used in the photometric model.

Magnetic Model of the Shutter

The shutter electromagnetics can be approximated quite well by a 2D magnetostatic model for the following reasons.

(i) The device has three magnet-coil combinations which are symmetrical about the circumference. Only one needs to be analyzed.

(ii) The magnets and coils have a constant depth radially and the flux that does work travels on cylindrical shells.

(iii) There is only one mechanical degree of freedom.

(iv) Only tangential forces can do work.

(v) The magnets are rigidly attached to the rotor so that they can do no work against each other.

(vi) The velocity of the magnet has a negligible effect on the field.

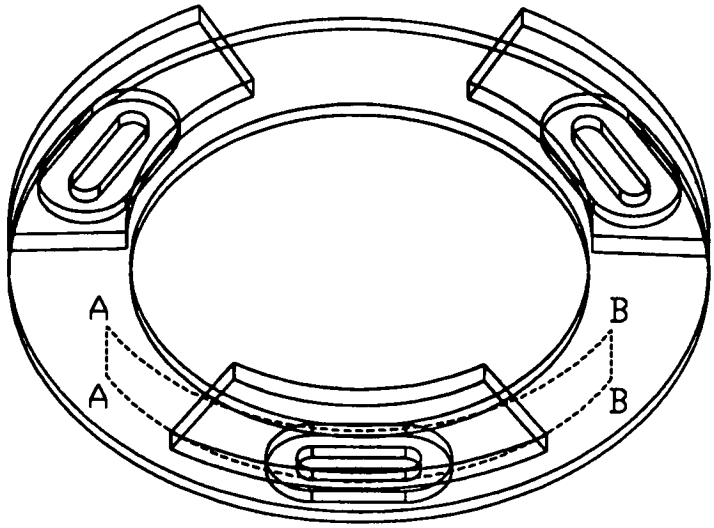

Figure 11. 3D view of the magnets, coils and lower fluxplate.

The upper fluxplate has been removed for clarity.

The two dimensional model is obtained by taking a cylindrical slice through the center of the magnets for a single magnet-coil set as shown in Figure 11. The extent of the flux-plate in the 2D model (Figure 12) is sufficiently long that its exact length does not affect the **B** field solution as shown in Figure 14.

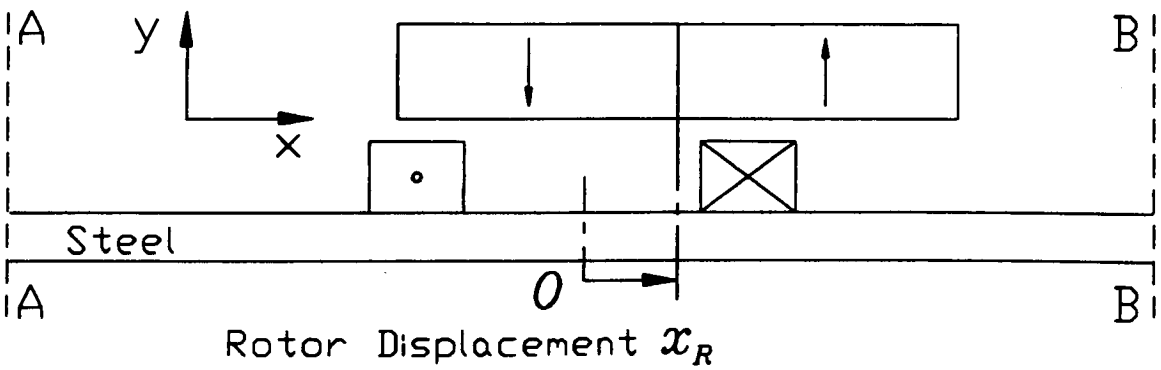

Figure 12. 2D approximation of the electromagnetics.

Table 2. Magnetic Model Data.

Magnetic material	Powdered metal NdBFe and epoxy
Remnance	5.5 kG
Coil turns	105
Coil current	2 amps
Depth of 2D Model	7.5 mm
R_{mag}	18.75 mm

While the 2D magnetic model will result in forces and displacements, the shutter mechanism will be modeled as a single degree of freedom rotational system where the applied magnetic force acting at a radius results in a torque and a rotational displacement, θ. The relationship between the circumferential displacement of the magnet, x_R, from the magnetic model and the rotation, θ (radians), of the mechanical model is

$$x_R = R_{mag} \cdot \theta \tag{46}$$

Similarly, the torque in the mechanical model is obtained as the force from the magnetic model multiplied by the radius R_{mag}.

Finite Element Solutions

Having established a magnetic model of the device, the magnetic force generated as a function of displacement can be obtained.

Opening: The coil current is on.

$F_x(\theta)$ provides the driving force to accelerate the moving parts and does work against the spring.

Closing: The coil current is off.

The driving force is the spring force $K \cdot \theta$.

F_x is assumed to be zero.

In order to evaluate the force generated as a function of displacement, the field solution will be obtained with the magnet positioned at points evenly spaced through its range of motion, then a numerical derivative will be evaluated at each point. The region has been meshed (Figure 13) with the appropriate material properties for each element.

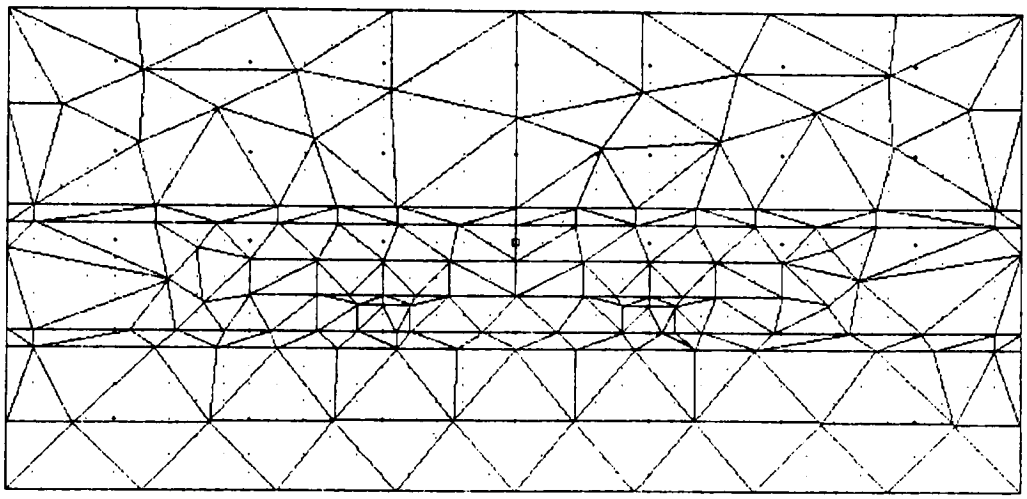

Figure 13. Finite element mesh for one magnet position.

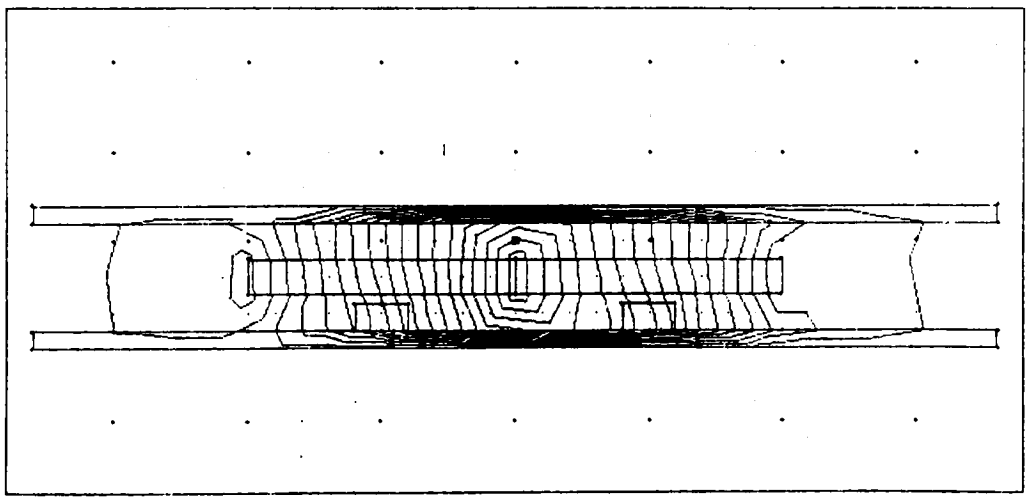

Figure 14. **B** field for one magnet position.

Numerical Derivatives

Once the field energy is obtained for a set of displacements, the gradient of those field energies needs to be determined in order to calculate the force in the direction of the displacement. This will be accomplished with two numerical differentiation schemes as outlined below.

Three-Point Derivative:

Centered: $$f'(x_0) = \frac{1}{2h}[f(x_0 + h) - f(x_0 - h)] + O(h^2). \tag{47}$$

One-sided: $$f'(x_0) = \frac{1}{2h}[-3f(x_0) + 4f(x_0 + h) - f(x_0 + 2h)] + O(h^2) \tag{48}$$

where the left end derivative is obtained with h positive and the right end derivative is obtained with h negative.

Force Results

A commercial magnetostatic finite element code called Maxwell from Ansoft Corporation was used to model the magnetics of the shutter. Ten finite element field solutions were obtained with the permanent magnet in ten positions along the travel of the magnet. The field energy is calculated from Equation (29) by the difference of two integrals. The magnetostatics software is capable of calculating these integrals directly from the field solution. When these quantities are subtracted, the energy function is available for numerical differentiation. The results are shown in Table 3, the energy has been plotted in Figure 15 and the force plotted in Figure 16.

Table 3. Finite Element Results.

Model depth			7.50 mm		
x_R (mm)	$\frac{1}{2}\int \mu H^2 dxdy$ (J/mm)	Error Estimate	$\int JA dxdy$ (J/mm)	Energy (J/mm)	Force (N)
-0.5	1.7488	0.0076	0.0756	1.6732	0.2981
0	1.7465	0.0054	0.0511	1.6954	0.3693
0.5	1.7489	0.0081	0.0265	1.7224	0.3665
1	1.7468	0.0044	0.0025	1.7443	0.3414
1.5	1.7478	0.0061	-0.0201	1.7679	0.3222
2	1.7470	0.0076	-0.0403	1.7873	0.2621
2.5	1.7465	0.0058	-0.0564	1.8029	0.2091
3	1.7480	0.0053	-0.0671	1.8151	0.1270
3.5	1.7482	0.0052	-0.0716	1.8198	0.0217
4	1.7480	0.0078	-0.0700	1.8180	-0.0752

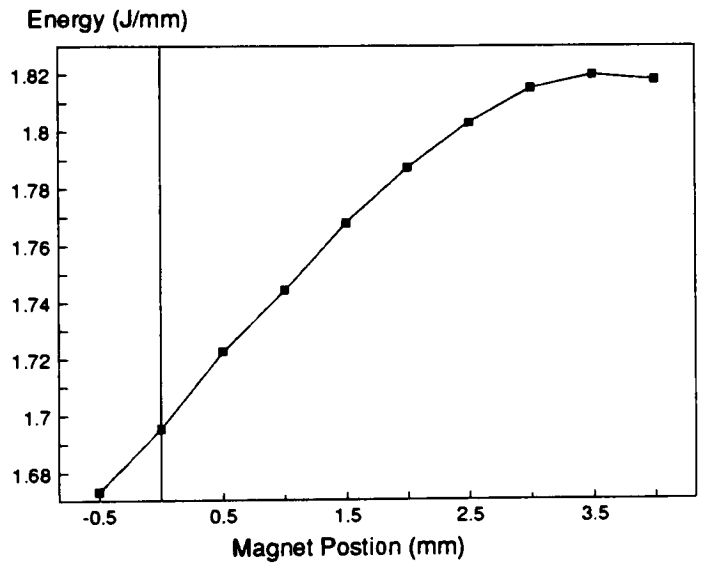

Figure 15. Energy of field vs magnet position.

Thus the force from a single magnet-coil pair has been calculated. This force is multiplied by three to obtain the total force acting on the rotor, which is used in the mechanical model of the shutter.

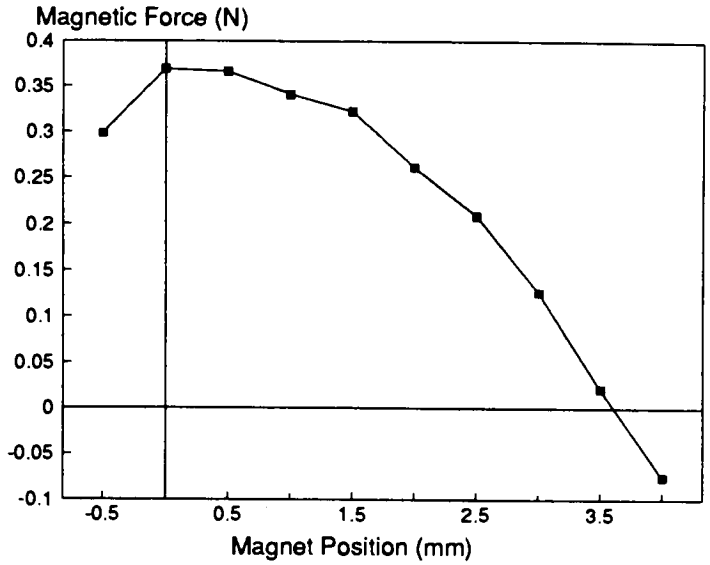

Figure 16. Magnetic force vs magnet position.

Mechanical Model of the Shutter

The shutter consists of a mechanism that contains three blades and a rotor as the only moving parts. These are lumped into a single equivalent inertia, $I^*(\theta)$. The section below details how this equivalent inertia is calculated. There are only three forces exerting torques on this inertia: the magnetic force at a given radius, a spring force acting at a given radius, and friction that has been modeled as viscous friction. Therefore the shutter is analogous to a rotationally-forced mass-spring-damper system modeled by the familiar second order differential equation.

$$I\ddot{\theta} + C\dot{\theta} + K\theta = T \tag{49}$$

The torque T results from the magnetic forces calculated from the magnetic model. The actual equation of motion is fully developed in the sections that follow. Its solution provides position-time information for the mechanical model, but additional analysis is required to establish the final shutter model.

Equivalent Inertia Calculation

Measured Inertia

The rotor is a complex part with many different materials: a polycarbonate base, three epoxy bonded powdered metal magnets, and steel pins to actuate the three blades. The inertia of the part was measured using a "Space Electronics Inc. Series 5000 Moment of Inertia Measuring Instrument." This instrument works by timing the period of oscillation of the inverted torsional pendulum on which the part to be measured is attached. The rotor axis was easily aligned with the axis of rotation of the torsional pendulum.

Mass Moment of Inertia of Rotor: 0.000186 in-oz-sec^2.

Converting to cgs units in which the problem will be analyzed gives,

$$I_{rotor} = 13.1345 \text{ g} \cdot \text{cm}^2 \tag{50}$$

Calculated Inertia

The moment of inertia of the blade about its centroid was calculated using the analysis available on the Unigraphics II CAD system.

Table 4. Blade Inertia Data.

Shutter Blade Data	Value	Symbol
Material	Mylar	
Thickness	0.22 mm	
Density (area)	0.02923 g/cm^2	
Mass	0.085675 g	M
Centroidal Moment of Inertia	0.08875 g · cm^2	I_B
Radius (Moving Pin to Centroid)	15.416 mm	R_B
Radius (Axis to Moving Pin)	21.25 mm	R_m
Radius (Axis to Fixed Pin)	18.1 mm	R_f

Equivalent Inertia of Linkage

The geometry of the rotor and one shutter blade is shown in Fig 17.

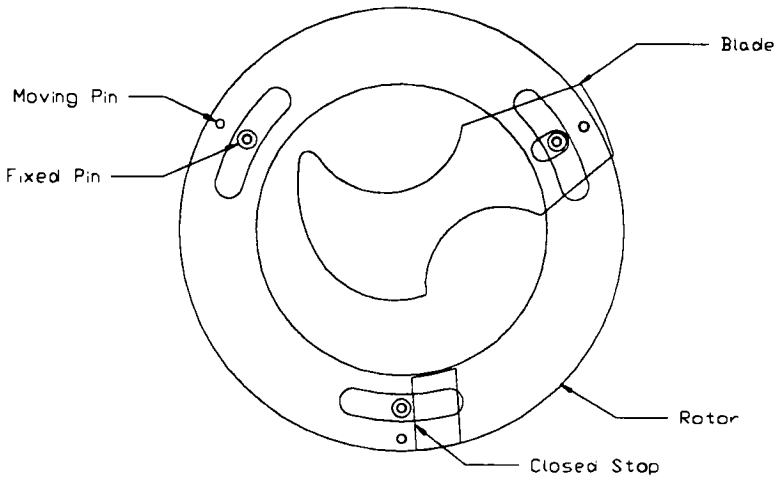

Figure 17. Geometry of rotor and one shutter blade.

The system of rotor and blades may be simplified to an equivalent single degree of freedom system with the rotor angle θ as the input. This is achieved by equating the kinetic energy of the blade with the kinetic energy of an equivalent blade inertia at the rotor speed by use of an influence coefficient.

The following linkage represents the rotor-blade system (Figure 18).

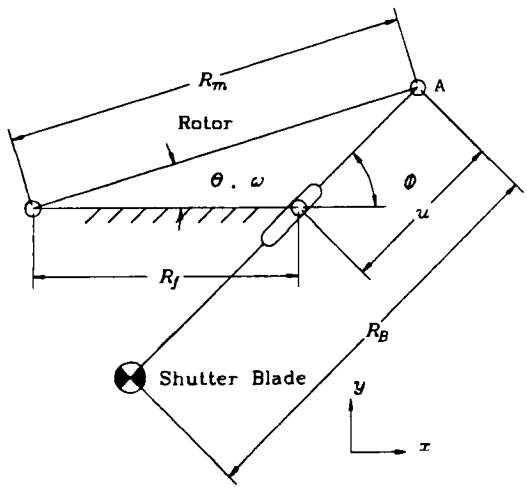

Figure 18. Equivalent linkage for rotor and one shutter blade.

The blade has a centroidal moment of inertia I_B, mass M, and is rotating at $\dot{\phi}$ while translating with $\dot{u}$.

Both ϕ and u are known functions of θ. If point A corresponds to the moving pin, and the relative position of A from the fixed pin is given by A_x and A_y, then the functions are given by

$$\begin{aligned} \phi(\theta) &= \angle(A_x, A_y) \\ u(\theta) &= \sqrt{A_x^2 + A_y^2} \end{aligned} \tag{51}$$

where

$$\begin{aligned} A_x &= R_m \cdot \cos(\theta) - R_f \\ A_y &= R_m \cdot \sin(\theta) \end{aligned}$$

The kinetic energy of the blade is

$$KE_B = \frac{1}{2}(Mv^2 + I_B\dot{\phi}^2) \tag{52}$$

where v is the speed of the blade centroid. However,

$$\dot{\phi} = \frac{d\phi}{d\theta}\frac{d\theta}{dt} = \frac{d\phi}{d\theta}\omega \tag{53}$$

and the speed squared of the blade centroid is

$$\begin{aligned} v^2 &= \dot{u}^2 + \dot{\phi}^2(R_B - u)^2 \\ &= \left(\frac{du}{d\theta}\right)^2\omega^2 + \left(\frac{d\phi}{d\theta}\right)^2\omega^2(R_B - u)^2 \end{aligned} \tag{54}$$

Thus the kinetic energy of the blade resulting from the rotor motion is

$$\mathrm{KE}_{eq} = \frac{1}{2} I_{eq} \omega^2 \tag{55}$$

where the equivalent inertia of one blade is given by

$$I_{eq} = M\left(\left(\frac{du}{d\theta}\right)^2 + \left(\frac{d\phi}{d\theta}\right)^2 (R_B - u)^2\right) + I_B\left(\frac{d\phi}{d\theta}\right)^2 \tag{56}$$

Equation (56) has been calculated numerically and is included in Appendix 2. A graph showing the result of that calculation is shown in Figure 19.

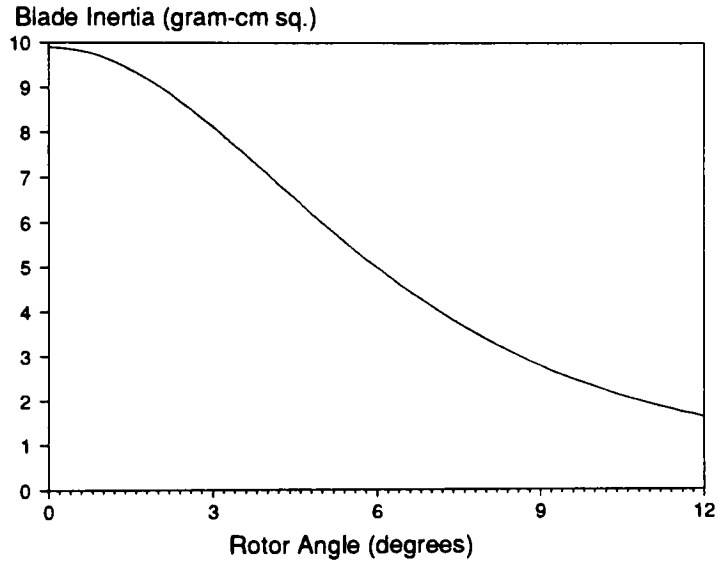

Figure 19. Equivalent inertia of blade.

There are three blades and a rotor with the magnets attached. The measured moment of inertia of the rotor is given above. The inertia of the spring will be neglected. Thus the system inertia referenced to the speed of the rotor is

$$I^*(\theta) = I_{\text{rotor}} + 3I_{eq}(\theta) \tag{57}$$

and the multibody system has conveniently been reduced to a single degree of freedom system with an inertia dependent on position.

The value of $I^*(\theta)$ will be numerically calculated and tabulated in a manner similar to the electromagnetic force components. These tables will then be interpolated during the integration of the equations of motion.

Equations of Motion

A simplified model of a forced rotating mass, spring and damper was introduced above using Equation (49). The inertia of the mass is represented by the system inertia, $I^*(\theta)$. The spring that acts on the rotor has a preload force to keep the shutter closed when the rotor has an angular position of zero. This is present in the model as a constant θ_s.

Opening

When the drive current is on, the torque acting on the system is the magnetic force acting at a given radius. Thus the equation of motion for the forced rotational mass-spring-damper is given by

$$I^*(\theta)\ddot{\theta} + C\dot{\theta} + K(\theta + \theta_s) = R_{mag} \cdot F_x(\theta) \tag{58}$$

The variable inertia and force have been calculated above. The viscous damping coefficient C is a small constant. The spring stiffness K is a constant. R_{mag} is the radius of the center of the magnets where the 2D force is calculated. Initial conditions are zero angular position and velocity of the rotor. The force is present at time zero for as long as the current is on. The current turns off at a predetermined time at which point the equation of motion becomes the closing equation of motion.

Closing

At the predetermined time, t_c, the current creating the opening force turns off and the resulting equation of motion is

$$I^{\cdot}(\theta)\ddot{\theta} + C\dot{\theta} + K(\theta + \theta_s) = 0 \tag{59}$$

with only the spring driving the shutter system to a closed configuration.

Limits of Motion

If the current is turned on for a long enough time, the travel of the rotor will exceed the allowable travel of the rotor. There are stops built onto the assembly at the closed end and the full open end of the travel of the rotor. The rotor bounces off its stops and this must be included in the simulation.

The bounce will be modeled with a coefficient of restitution, e, such that the velocity after the bounce $\dot{\theta}_{final}$ is found from $\dot{\theta}_{initial}$, the velocity before the bounce by the relation

$$\dot{\theta}_{final} = -e \cdot \dot{\theta}_{initial} \tag{60}$$

The value for e is adjusted to obtain an amplitude for the first bounce that approximates the bounce observed in an actual shutter. Figure 20 shows the data collected from one run of the ACSL shutter model where the drive time is .05 seconds. This clearly shows the presence of opening and closing bounce of the mechanism that represents what is seen in practice.

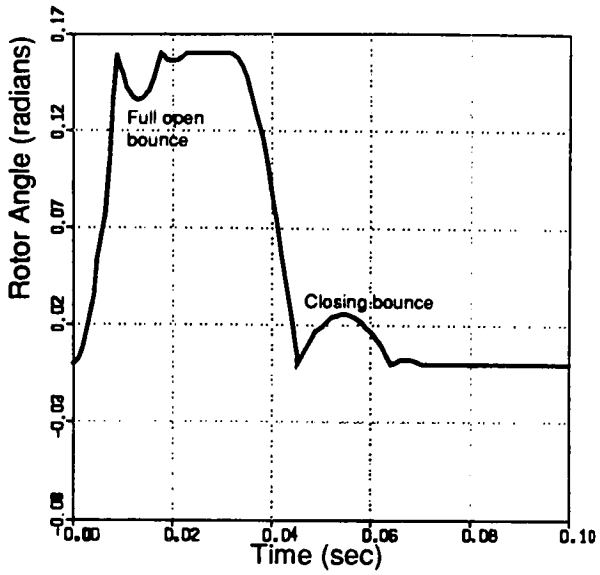

Figure 20. One run of the model with a long drive time showing the bounce behavior.

Photometric Model of the Shutter

The last step to completing the shutter modeling is to use the position of the mechanism to find the opening of the blades versus time and to then calculate the resulting photographic exposure. It is at this point that the behavior of the system is revealed in the characteristic exposure program.

Aperture Area vs Rotor Angle

The primary quantity of interest for the application is not angular position of the rotor but exposure. Once the position is known, the area of the aperture is referenced from a table that is interpolated linearly. In this way, a graph of area-versus-time may be calculated along with the position-time curve. The area under the area-time curve is then calculated to estimate the total exposure.

The area of the aperture opening as a function of rotor angle (Figure 22) was created by assembling the blades to the stator and rotor pins in the CAD system for a set of rotor angles. The blade edges were then trimmed to create a closed curve whose area could be measured using the CAD system (Figure 21).

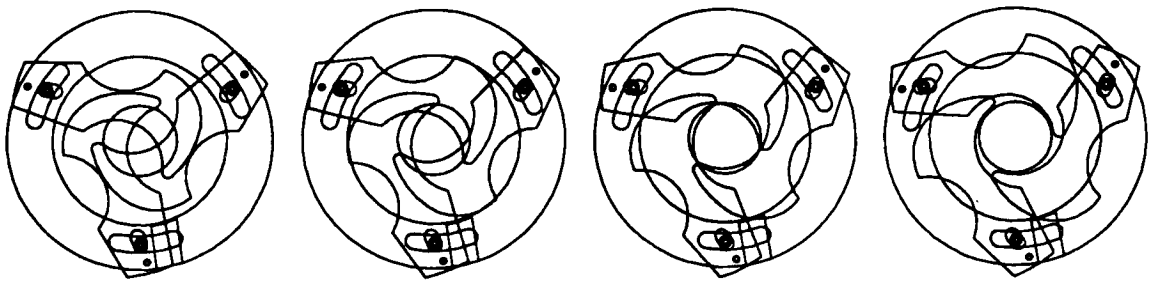

Figure 21. Four of the eight layouts used to derive aperture area versus rotor angle.

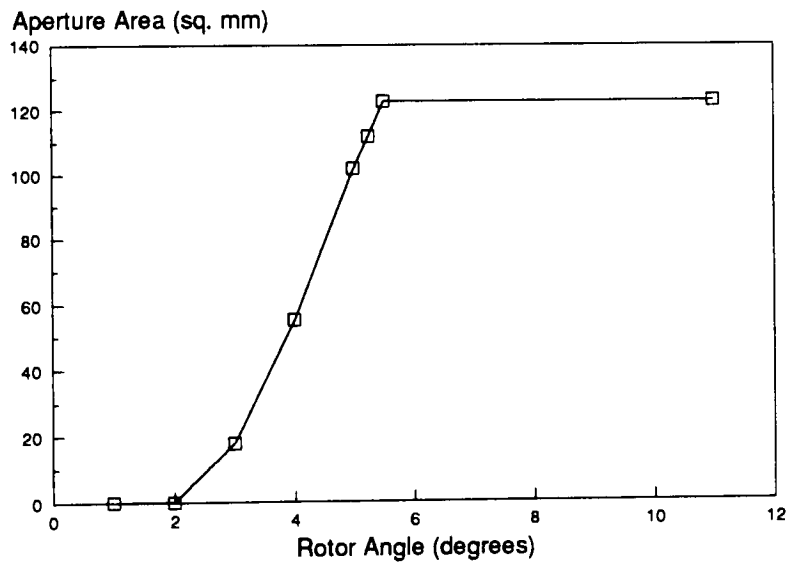

Figure 22. Aperture area versus rotor angle.

A characteristic of shutter blades is overtravel. Blades are designed to keep closing beyond the point at which the area of the opening becomes zero and keep opening beyond the point at which the full diameter of the lens opening is revealed. Overtravel serves several important functions. It helps to assure that the blades will not leak light when closed, it prevents bounce of the mechanism from creating a second exposure, and

it allows the mechanism to accelerate to a significant velocity before beginning the exposure so that the total time the shutter is open is reduced. A plot of aperture area vs time overlaid on the position-time curve shows the effect of overtravel (Figure 23). Note that the bounce of the mechanism at full open and closing is not present in the area curve due to the overtravel of the blades.

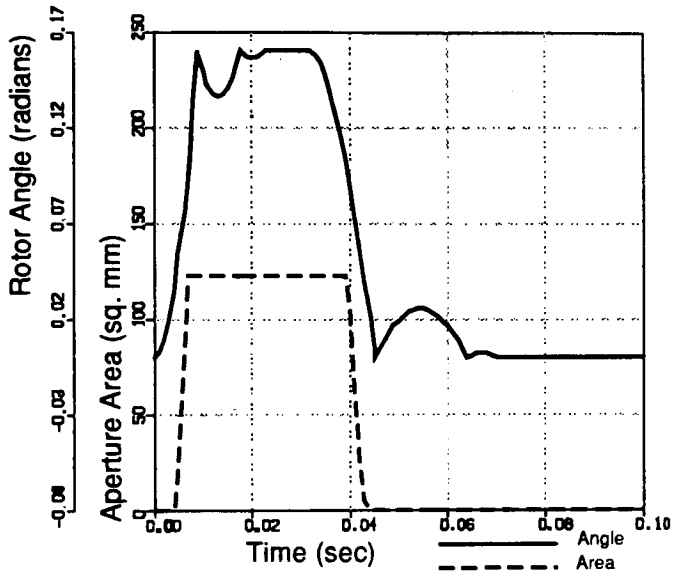

Figure 23. The aperture area overlaid on the position-time plot shows the effect of overtravel.

Integration of the Differential Equations of Motion

The equation of motion described by Equation (58) is a non-linear equation because of the dependency of inertia and force on position. Furthermore, the equation has discontinuities when the limit stops are reached in the solution or when the current is turned off. These factors make it very difficult to obtain a closed-form solution, therefore the equation will be solved numerically.

There are several numerical techniques for solving such equations. Runge-Kutta is a particularly robust method. It was initially used on this problem, but the presence of discon-

tinuities gave the variable step size implementation some difficulty. Ideally, the integration should restart with new initial conditions on the other side of any discontinuity.

A high-level language called ACSL (Advanced Continuous Simulation Language) [20] is available which already provides for the automatic restarts of differential equations at each occurrence of an event that represents a discontinuity, such as a bounce.

ACSL Model

The ACSL code appears in Appendix 3. It has three basic sections.

Initial Section

The initial section contains constants and initial conditions. The ACSL model contains three tables for the force vs angle (Figure 16), system inertia vs angle (Figure 19) and aperture area vs angle (Figure 22).

Dynamic Section

The dynamic section contains the Derivative section which contains the dynamic model and is calculated at every time step of the integration. Following the Derivative section is the Discrete section that contains statements that are executed only when an event occurs. This is the unique advantage of using ACSL to place discontinuities in the integration. There is a Discrete section for bounce at the bottom of the travel, bounce at the top of the travel, a section called XMAX to capture the maximum aperture achieved, and two sections COL and COLL to capture the time the shutter first opens and the time the shutter finally closes.

Terminal Section

The terminal section contains statements that are executed once at the end of a simulation. Total open time is calculated here.

Model Output

To simulate a shutter system, the same measurements that are made with an oscilloscope must be made on the dynamic model. The area under the aperture-area-vs-time curve is a measure of exposure and is readily determined since ACSL is designed to integrate quantities. The aperture area, A, of the shutter is in a look up table of angular position called AREA so the area under the aperture-area-vs-time curve is simply executed as

```
A       = AREA(X)
SUMA    = INTEG(A, 0.0)
```

where X is the angular position of the rotor and 0.0 is the initial condition. This value needs to be transformed to EV.

The total time open (TT) is output by capturing the first time that the shutter opens and the last time it closes, which accounts for any re-opening due to bounce. The maximum aperture achieved is output to calculate AV.

Two ACSL models have been created and run. The first model (Appendix 3) consists of code to take a single exposure which was useful for debugging the code and adjusting parameter values. While in the ACSL environment, the model may be run numerous times while any parameter value is changed. After each run, quantities calculated during the simulation can be displayed or plotted. The second model is the same as the first model with statements added (Section 8.1, ACSL Reference Manual) to execute a parameter sweep on drive time (OT). In this way the exposure program of the shutter is easily obtained by running the simulation where the code repeatedly increases the time

geometrically during which the current is on. Figure 24 shows the angle (position) versus time curves and Figure 25 the corresponding aperture versus time curves for three of the data points that make up one exposure program sweep.

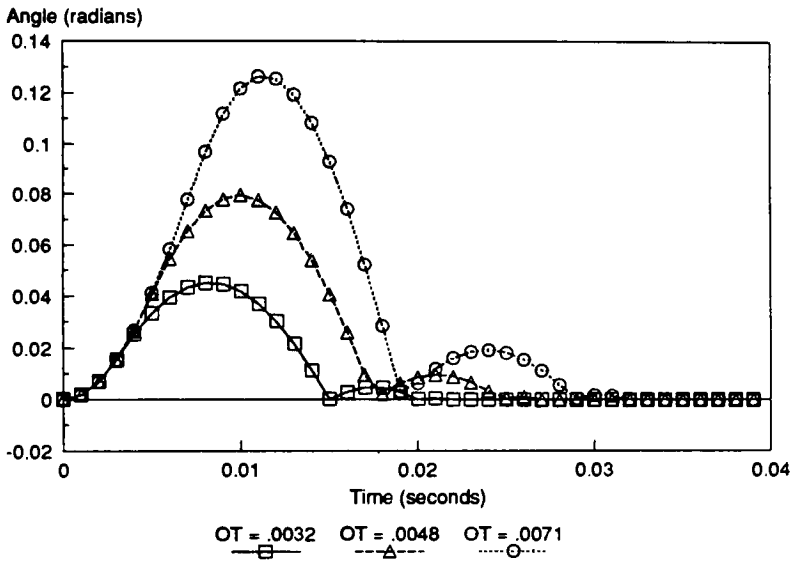

Figure 24. Position curves for three drive times.

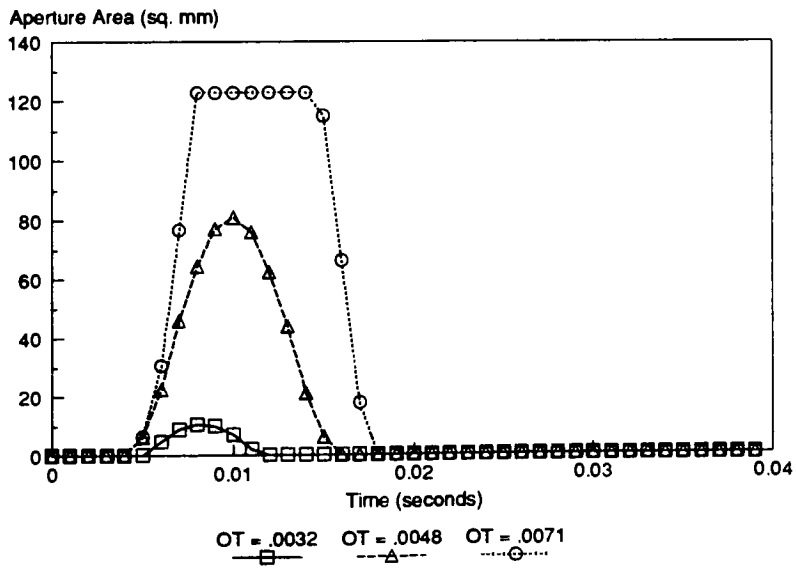

Figure 25. Corresponding aperture curves.

One of the benefits of building a model is rapid evaluation of the effect of changes in a parameter. The spring rate, SK, appears in the ACSL model and so the sweep has been repeated for three values of SK and the resulting data is shown in Figure 26. Note that extensive computation is done to obtain a graph like this since each data point represents an exposure and each exposure consists of computations over hundreds of time step increments.

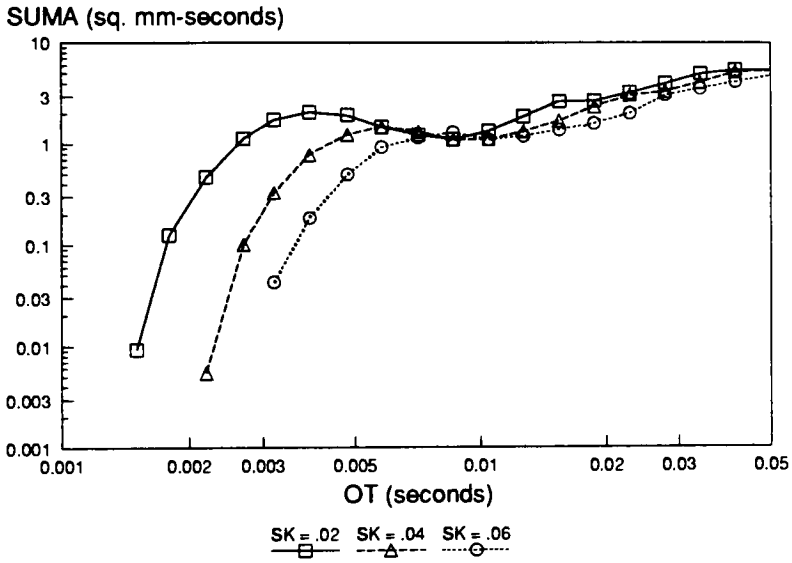

Figure 26. Area under the aperture vs drive time curve for 3 springs.

Of the three springs, SK = .06 appears to be the best choice because it is less sensitive to drive time at low areas and does not contain a negative slope like the curve for SK = .02 has in the middle of the graph. Though SUMA is the quantity calculated by the model, it needs to be transformed into Exposure Value in order to report results in photometric quantities.

High EV corresponds to a small area under the shutter trace curve. Doubling the area under the curve would result in a one stop change in exposure or a reduction of one EV. Therefore a relative EV is calculated from the area, SUMA (sq. mm-seconds) by the function

$$EV = \frac{-\log(SUMA)}{\log(2)} + C \tag{61}$$

where C is a constant used to correct the offset in the value of EV to make it an absolute EV. The value of C may be adjusted until the relative EV matches the absolute EV calculated from the sum of the AV and TV as explained below.

The area under the curve for the actual shutter trace is made into a rectangular area for the purpose of dividing the area's exposure between an aperture and a shutter speed (Fig 9). Although the aperture varies continuously during any exposure (except when full open), it is useful to assign a single aperture to the exposure since aperture affects picture sharpness. The definition chosen here is to use the maximum aperture attained during the exposure. This value is captured during the simulation as AMAX. In order to calculate AV, the lens focal length is needed. It is assumed that the focal length is 35 mm. The maximum area of the aperture is converted into the diameter of a circle of equal area and the f-number is calculated using the focal length over the diameter. Equation (62) converts AMAX into an f-number, then AV is calculated from A using Equation (38).

$$A = \frac{35}{\sqrt{\left(\frac{4 \times AMAX}{\pi}\right)}} \tag{62}$$

The effective shutter speed that results in the same area under the rectangular trace, as the area under the actual shutter trace is simply[1]

$$t_{eff.} = \frac{SUMA}{AMAX} \tag{63}$$

1 If data were collected from a prototype on an oscilloscope, SUMV in volt-seconds would be divided by VMAX in volts to give the effective shutter speed. VMAX is then multiplied by a coefficient with units of sq.mm per volt to yield AMAX.

since the units for SUMA are $mm^2 \cdot sec$ and the units for AMAX are mm^2.

An effective TV can be calculated from the effective shutter speed using Equation (35). Now that AV and TV have been calculated, their sum represents EV which is shown in Table 5.

Table 5. Results from Shutter Simulations.

OT (msec)	TT (msec)	AMAX (mm^2)	SUMA ($mm^2 \cdot sec$)	$t_{eff.}$ (msec)	A	AV	TV	EV
2.75	0.00	0.00	0.0000					
2.85	2.63	1.80	0.0032	1.75	23.10	9.06	9.16	18.22
2.89	3.50	3.24	0.0076	2.33	17.22	8.21	8.74	16.96
3.03	4.76	6.15	0.0195	3.17	12.50	7.29	8.30	15.59
3.18	5.92	9.84	0.0387	3.93	9.89	6.61	7.99	14.60
3.34	6.67	12.81	0.0566	4.42	8.67	6.23	7.82	14.05
3.51	7.59	17.30	0.0870	5.03	7.46	5.80	7.64	13.43
3.69	8.23	24.55	0.1221	4.97	6.26	5.29	7.65	12.94
3.87	8.89	34.02	0.1772	5.21	5.32	4.82	7.58	12.41
4.06	9.45	43.51	0.2404	5.53	4.70	4.47	7.50	11.97
4.27	9.92	52.94	0.3087	5.83	4.26	4.18	7.42	11.61
4.48	10.33	64.07	0.3839	5.99	3.88	3.91	7.38	11.29
4.70	10.72	77.06	0.4768	6.19	3.53	3.64	7.34	10.98
4.94	11.03	88.52	0.5636	6.37	3.30	3.44	7.30	10.74
5.19	11.41	103.79	0.6863	6.61	3.04	3.21	7.24	10.45
5.44	11.69	115.40	0.7883	6.83	2.89	3.06	7.19	10.25
5.72	12.02	122.70	0.9064	7.39	2.80	2.97	7.08	10.05
6.00	12.30	122.70	0.9868	8.04	2.80	2.97	6.96	9.93
6.30	12.57	122.70	1.0502	8.56	2.80	2.97	6.87	9.84
6.62	12.81	122.70	1.1023	8.98	2.80	2.97	6.80	9.77
6.95	13.03	122.70	1.1471	9.35	2.80	2.97	6.74	9.71
7.30	13.28	122.70	1.1942	9.73	2.80	2.97	6.68	9.65
7.66	13.53	122.70	1.2382	10.09	2.80	2.97	6.63	9.60
8.04	13.72	122.70	1.2710	10.36	2.80	2.97	6.59	9.56
8.45	13.94	122.70	1.3066	10.65	2.80	2.97	6.55	9.52

Results are for SK = .06.

Predicted Exposure Program

The results of the simulation with SK = .06 have been transformed to EV using Equation (61) and plotted in Figure 27 to show the drive time needed for a given exposure relating to this shutter.

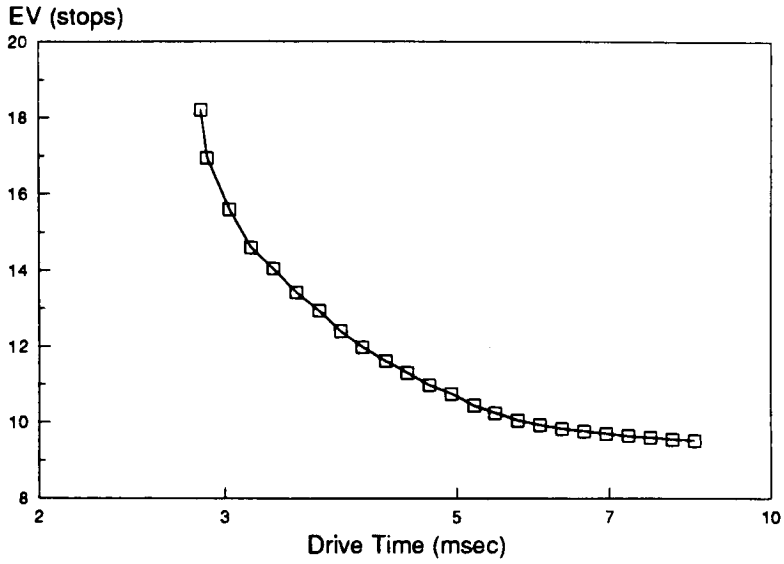

Figure 27. Predicted exposure versus drive time.

If the Aperture Value is plotted against the Time Value, the characteristic behavior of the dynamics of this shutter are revealed in the exposure program shown in Figure 28.

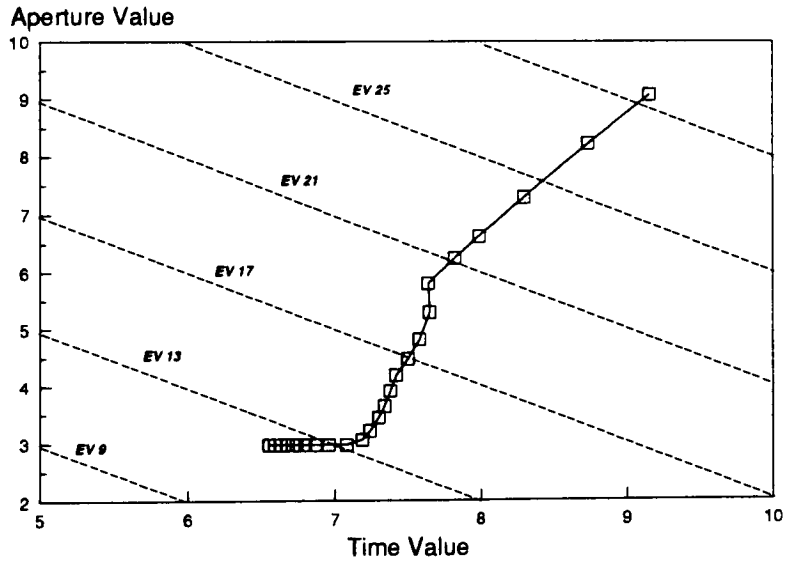

Figure 28. Predicted exposure program.

VI Results and Conclusions

Characteristics of this shutter

The EV versus drive time chart shown in Figure 27 shows that this shutter is capable of achieving the 8 stops of exposure range required. The behavior is not ideal, because the shutter EV is very sensitive to drive time at short drive times. The AV versus TV chart of Figure 28 shows that the change in aperture is largely responsible for the change in EV.

For long drive times, there is a distinct horizontal region in the exposure program at lower values of EV where the shutter is driven to the stop and held there until the drive current is turned off. The shutter attains its maximum aperture of *f*/2.8 and any increase in EV is due to longer shutter open times (smaller TV values). An example of this behavior is shown in Figure 23. Unfortunately, these long drive times result in shutter open times that are unacceptably long, where camera shake and subject motion become a problem.

Uses for the Model

The value in building such a model is to gain insight into the behavior of the system and to look for areas where the design can be improved. From the finite element results, flux lines are visualized (Figure 14) that may show where flux leakage is occurring. Implementing a different design for the flux path can improve performance. The equivalent inertia calculation shows that the system inertia is high at the start of the travel (Figure 19). The model allows experiments to be performed to look at the effect of this inertia

profile compared to a system inertia that is low at the start of the travel. If the performance change is favorable, a redesign of the linkage may be attempted that results in an improved inertia profile. The blade geometry creates an area versus position profile (Figure 22) that is available as a design variable. Indeed this has been exploited in cameras to make the system less sensitive to drive time at high EV settings. Availability of such a model allows new blade geometries to be readily tested. If a design variable appears explicitly as a variable in the ACSL model, study of the effects of changes in that variable are very easy to accomplish. This was demonstrated for the case of the spring constant, SK.

This analysis has focused on an open loop shutter by predicting the drive times needed to achieve a given EV. This model could serve as the "plant" in a closed loop control simulation of the same shutter once sensor behavior and a control system are added to the shutter dynamic model.

This shutter used a drive current that was only on or off. The model could easily evaluate the effect of making the current bipolar and driving the shutter closed with magnetic forces as well as spring forces.

Typically, a math model is used to understand the behavior of a device, so model parameters are adjusted to correlate it with experimental data. Once confidence in the model is established, it may be used to evaluate many of the design and noise parameters that affect performance.

Improvements to the Model

There have been advancements in commercial magnetic finite element codes in the last few years. It is now possible to do three dimensional magnetic models. These are neces-

sarily larger and more difficult to create, but may yield more accurate answers. The steel was assumed to be below saturation in this analysis. Magnetostatic codes that can model saturation are available. When the design indicates that the steel is used in the non-linear part of its B-H curve, a non-linear analysis is required. However, solution times can be an order of magnitude longer because of the iterative nature of a non-linear solution. Another way to improve the accuracy of the magnetic force is to measure it and use experimental data in the model.

Friction can be a significant percentage of the total force acting in the system and could be added to the model. The ACSL manual has an example problem (A-13) where friction dominates the behavior of the system. However if this technique is applied to the shutter model, the simulation will take significantly longer to run as many more events will be added to the event list.

This model is a single degree of freedom system, but in reality there are clearances in the linkage that are not accounted for. Although these are small, it would be possible to model them with a multibody analysis code like ADAMS.

The electric circuit has been simplified in this model. The current is assumed to turn on and off instantaneously. The large inductances of the drive coils make this impossible in real circuits. An improved model would have a pair of coupled differential equation for the circuit which includes the inductance terms.

Conclusion

A procedure that can be followed to analyze the behavior of many types of leaf shutter systems has been developed. Methods to calculate the magnetic force, the system inertia, and the aperture-area versus position profile have been explained. The results of these

calculations are used to develop a dynamic shutter simulation. A method to transform the results of the dynamic simulation to photometric quantities for shutter system evaluation has been presented. The model makes the study of some design parameters very easy, as was demonstrated in the case of a spring constant. Valuable insight into the behavior of the shutter system is gained by following the steps in this procedure.

VII References

1 P. Silvester and M. V. K. Chari, "Finite Element Solution of Saturable Magnetic Field Problems," *IEEE Trans. Power Apparatus and Systems,* vol. PAS-89, no. 7, pp. 1642-1648, September/October 1970.

2 J. R. Brauer, "Finite Element Analysis of Electric and Magnetic Fields," First Chautauqua on FEM, pp. 367-379.

3 E. Guancial and S. DasGupta, "Three-Dimensional Finite Element Program for Magnetic Field Problems," *IEEE Trans. Magnetics,* vol. MAG-13, no. 3, pp. 1012-1015, May 1977.

4 J. Simkin and C. W. Trowbridge, "On the Use of the Total Scalar Potential in the Numerical Solution of Field Problems in Electromagnetics," *Int. J. Num. Met. Eng.,* vol. 14, pp. 423-440, 1970.

5 C. Magele, H. Stœgner and K. Preis, "Comparison of Different Finite Element Formulations for 3D Magnetostatic Problems," *IEEE Trans. Magnetics,* vol. 24, no. 1, January 1988.

6 I. D. Mayergoyz, M. V. K. Chari and J. D'Angelo, "A New Scalar Potential Formulation for Three-Dimensional Magnetostatic Problem," *IEEE Tran. Magnetics,* vol. MAG-23, no. 6, November 1987.

7 P. P. Silvester and R. L. Ferrari, "Finite Elements for Electrical Engineers," Cambridge University Press, 1983.

8 K. Reichert, "The Calculation of Magnetic Circuits with Permanent Magnets by Digital Computers," *IEEE Trans. Magnetics,* vol. MAG-6, no. 2, pp. 283-288, June 1970.

9 F. A. Fouad, T. W. Nehl and N. A. Demerdash, "Permanent Magnet Modeling for use in Vector Potential Finite Element Analysis in Electrical Machinery," *IEEE Tran. Magnetics,* vol. MAG-17, no. 6, November 1981.

10 C. S. Biddlecombe and J. Simkin, "Enhancements to the PE2D Package," *IEEE Trans. Magnetics,* vol. MAG-19, no. 6, pp. 2635-2638, November 1983.

11 M. Marinescu and N. Marinescu, "Numerical Computation of Torques in Permanent Magnet Motors by Maxwell Stresses and Energy Method," *IEEE Trans. Magnetics,* vol. 24, no. 1, pp.463-466, January 1988.

12 J. L. Coulomb and G. Meunier, "Finite Element Implementation of Virtual Work Principle for Magnetic or Electric Force and Torque Computation," *IEEE Trans. Magnetics,* vol. MAG-20, no. 5, pp. 1894-1896, September 1984.

13 D. Tesar and G. K. Matthew, "The Dynamic Synthesis, Analysis, and Design of Modeled Cam Systems," Lexington Books, 1976

14 G. L. Elliott, "A Numerical Method for Predicting the Dynamic Performance of Electromechanical Relays," *Trans. ASME, J. Applied Mechanics*, pp. 360-362, June 1974.

15 B. Ancelle, J. L. Coulomb and B. Morel, "Implementation of a Computer Aided Design System for Electromagnets in an Industrial Environment," *IEEE Trans. Magnetics,* vol. MAG-16, no. 5, pp. 806-808, September 1980.

16 D. Howe and W. F. Low, "Design and Dynamic Calculations for Miniature Permanent Magnet Stepper Motors," *IEEE Trans. Magnetics*, vol. MAG-20, no. 5, pp. 1768-1770, September 1984.

17 B. D. Cullity, "An Introduction to Magnetic Materials," Addison-Wesley, 1972.

18 Lowther and Silvester, "Computer-Aided Design in Magnetics," Springer-Verlag, 1989.

19 J. N. Reddy, "An Introduction to the Finite Element Method," McGraw-Hill, 1984.

20 Mitchell and Gauthier Associates, "ACSL Reference Manual," Edition 4.1, 1987

VIII Appendix 1

Maximum Opening of Shutter Blade

DATA

$R_m := 21.25$

$R_f := 18.1$

$u_{max} := 4.75 + 1.2 - .975$

UNITS

$rad \equiv 1$

$deg \equiv \frac{\pi}{180}$

Initial guess: $\theta := 10 \cdot deg$

Maximum rotation of rotor

$$\theta_{max} := root\left[u_{max} - \sqrt{\left[R_m \cdot \cos(\theta) - R_f\right]^2 + \left[R_m \cdot \sin(\theta)\right]^2}, \theta\right]$$

$\theta_{max} = 11.267 \cdot deg$

Maximum rotation of blade

$\phi(\theta) := angle\left[\left[R_m \cdot \cos(\theta) - R_f\right], \left[R_m \cdot \sin(\theta)\right]\right]$

$\phi_{max} := \phi\left[\theta_{max}\right]$

$\phi_{max} = 56.574 \cdot deg$

Figure 29. MathCAD calculation of maximum opening.

IX Appendix 2

Equivalent Inertia of a Linkage System

UNITS rad ≡ 1 deg ≡ $\frac{\pi}{180}$ Units are g and cm

DATA $R_f := 1.81$ $R_m := 2.125$ $R_B := 1.5416$ $TOL \equiv 10^{-3}$

$I_B := 0.08875$ $M := 0.085675$ $\theta_{max} := 12 \cdot deg$

INCREMENTS $N := 60$ $j := 1 \ldots N$ $\theta_j := \frac{j}{N} \cdot \theta_{max}$ Angles in radians

KINEMATIC RELATIONS

$A_x(\theta) := R_m \cdot \cos(\theta) - R_f$ $A_y(\theta) := R_m \cdot \sin(\theta)$

$\phi(\theta) := \text{angle}[A_x(\theta), A_y(\theta)]$ $u(\theta) := \sqrt{A_x(\theta)^2 + A_y(\theta)^2}$

DERIVATIVES - INFLUENCE COEFFICIENTS

Angle of Blade

$D\phi(\theta) := \frac{d}{d\theta}\phi(\theta)$

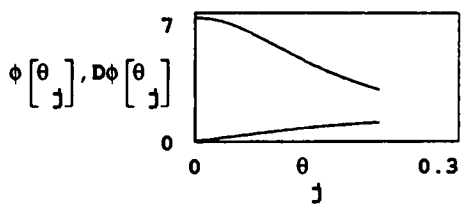

Position of Blade

$Du(\theta) := \frac{d}{d\theta}u(\theta)$

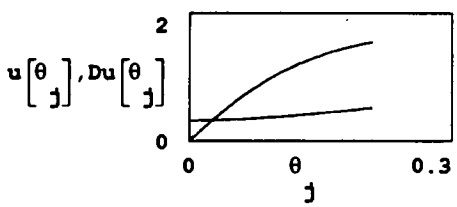

EQUIVALENT BLADE INERTIA

$I_{eq\_blade}(\theta) := M \cdot \left[Du(\theta)^2 + D\phi(\theta)^2 \cdot \left[R_B - u(\theta)\right]^2\right] + I_B \cdot D\phi(\theta)^2$

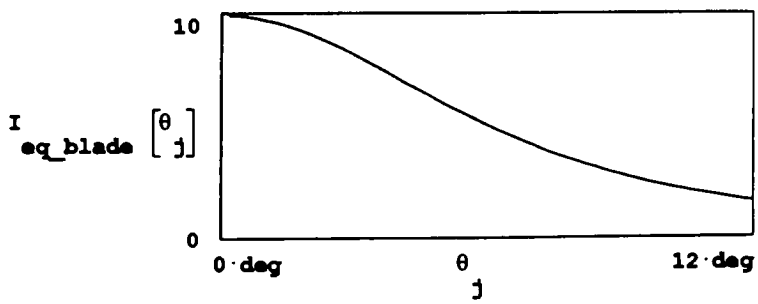

Figure 30. MathCAD calculation of system inertia.

X Appendix 3

ACSL Program

```
PROGRAM - S -
      "FIXED STEP, RESTITUTION, CURRENT IS ICUR"

INITIAL
      LOGICAL DUMP, LCOL, LXMAX

      DUMP = .FALSE.
      LCOL = .FALSE.
      LXMAX = .FALSE.

      "INTEGRATION CONSTANTS"
      CINTERVAL            CINT = 0.001
      NSTEPS               NSTP = 10
      CONSTANT             TSTP = 0.05
      CONSTANT             TINY = 1.0E-4

      "MODEL CONSTANTS"
      CONSTANT      RMAG = 0.01875        ,      RLB  = 0.01525
      CONSTANT      SK   = 0.5E-2         ,      THETAS = -0.1
      CONSTANT      THMIN = 0.0           ,      THMAX = 0.16
      CONSTANT      E    = 0.3            ,      OT   = 0.01
      CONSTANT      RD    = 57.29578
      CONSTANT      C    = 5.0E-5         ,      XCOL  = 0.0349

TABLE  FX, 1, 10 ...
  / -0.026667, 0.000000, 0.026667, 0.053333, 0.080000, ...
      0.106667, 0.133333, 0.160000, 0.186667, 0.213333, ...

      0.298108, 0.369311, 0.366510, 0.341406, 0.322178, ...
      0.262050, 0.209129, 0.127000, 0.021737, -0.075170 /

TABLE VEI, 1, 21 ...
   / 0.000000, 0.010472, 0.020944, 0.031416, 0.041888, ...
    0.052360, 0.062832, 0.073304, 0.083776, 0.094248, ...
    0.104720, 0.115192, 0.125664, 0.136136, 0.146608, ...
    0.157080, 0.167552, 0.178024, 0.188496, 0.198968, ...
    0.209440, ...
  4.28495E-06, 4.26026E-06, 4.18793E-06, 4.07339E-06, 3.92447E-06,
  3.75089E-06, 3.56210E-06, 3.36701E-06, 3.17324E-06, 2.98658E-06,
  2.81111E-06, 2.64935E-06, 2.50253E-06, 2.37089E-06, 2.25395E-06,
  2.15084E-06, 2.06042E-06, 1.98146E-06, 1.91264E-06, 1.85276E-06,
  1.80074E-06 /

"Aperture area (sq. mm) versus rotor angle (degrees)"
TABLE AREA, 1, 11 / 1., 2., 3., 4., 5., 6., 7., 8., 9., 11.27, 12.,
                    0.0, 0.0, 17.848, 55.123, 101.665, 157.718, ...
                    218.903, 275.813, 305.130, 314.159, 314.159 /

      "INITIAL CONDITIONS"
      XDIC = 0.0
      XIC = 0.0
```

```
      "CALCULATED CONSTANTS"
      XLL = THMIN - TINY
      XUL = THMAX + TINY
END $"OF INITIAL"

DYNAMIC
  DERIVATIVE
      SCHEDULE XMAX  .XP. (-XD)
      SCHEDULE COLL  .XP. (XCOL-X)
      SCHEDULE COL   .XP. (X-XCOL)
      SCHEDULE BOUNCB .XP. (XLL-X)
      SCHEDULE BOUNCT .XP. (X-XUL)
      PROCEDURAL(VFX = ICUR, X)
              IF (ICUR .LE. 0.5) GOTO CUROFF
                 "CURRENT IS ON"
                 VFX = FX(X)
                 GOTO DONE
              CUROFF..CONTINUE
                 VFX = 0.0
              DONE..CONTINUE
      END $"OF PROCEDURAL"
      ICUR = 1.0 - STEP(OT)
      FMAG  = RMAG*VFX
      SPRING = -SK*(X - THETAS)
      SUMFB = FMAG + SPRING - C*XD
      XDD   = (SUMFB)/VEI(X)
      XD    = INTEG(XDD, XDIC)
      X     = LIMINT(XD, XIC, XLL, XUL)
      A     = AREA(X*RD)
      SUMA  = INTEG(A, 0.0)
      TERMT (T .GE. TSTP)
  END $"OF DERIVATIVE"

      DISCRETE BOUNCB
              PROCEDURAL
              X = XLL
              XD = -E*XD
              CALL LOGD (.TRUE.)
              END $"OF PROCEDURAL"
      END $"OF BOUNCB"

      DISCRETE BOUNCT
              PROCEDURAL
              X = XUL
              XD = -E*XD
              AMAX = AREA(X*RD)
              LXMAX = .TRUE.
              CALL LOGD (.TRUE.)
              END $"OF PROCEDURAL"
      END $"OF BOUNCT"

      DISCRETE XMAX $"Capture A at first change in velocity"
      IF (LXMAX .EQ. .TRUE.) GOTO XMAX2
              AMAX = AREA(X*RD)
              LXMAX = .TRUE.
      XMAX2..CONTINUE
      END

      DISCRETE COL $"Capture time at first crack of light"
      IF (LCOL .EQ. .TRUE.) GOTO COL2
              TOPEN = T
              LCOL = .TRUE.
      COL2..CONTINUE
      END
```

```
    DISCRETE COLL $"Capture time at crack of light closing"
    TCLOSE = T
    END

      WRITE (11,200) T,A,ICUR
 200..FORMAT(3F20.4)
END $"OF DYNAMIC"
TERMINAL
TT = TCLOSE - TOPEN
WRITE (11,210) OT,TT,AMAX,SUMA
 210..FORMAT(/,F16.4,F20.10,F20.4,F20.4)
END
END
```